universität wien

DISSERTATION / DOCTORAL THESIS

Titel der Dissertation /
Title of the Doctoral Thesis

Mathematical Modelling of p62-Ubiquitin aggregates involved in cellular autophagy

verfasst von / submitted by

Julia Delacour

angestrebter akademischer Grad / in partial fulfilment of the requirements for the degree of

Doktorin der Naturwissenschaften (Dr.rer.nat.)

Wien, 2020 / Vienna, 2020

Studienkennzahl lt. Studienblatt / degree programme code as it appears on the student record sheet:	UA 796 605 405
Dissertationsgebiet lt. Studienblatt / field of study as it appears on the student record sheet:	Mathematik
Betreut von / Supervisor:	Univ.-Prof. Dr. Christian Schmeiser
Betreut von / Supervisor:	Prof. Dr. Marie Doumic

Thanks

First, I would like to thank my two PhD supervisors. I am very grateful towards Christian Schmeiser, who has given me the opportunity to work on this very beautiful and original subject. A lot of his ideas can be found again in this thesis. I thank him also for the patience and kindness he showed me during these last three years. I would like to thank Marie Doumic as well for her overall support throughout the three years.
I thank also Silvia Cuadrado and Mostafa Adimy for the time spent to review this thesis and their thoughful reports.
Furthermore, I would like to thank all the people that have helped me to deal with the administrative load coming with a PhD in co-tutelle. In Paris, Salima Lounici, Catherine Drouet, Malika Larcher and in Vienna, Cornelia Oppitz, Bettina Hiebl, Matteo Tommasini and Barbara Seiss.

Then, I would like to thank my colleagues. We have the chance in Paris at the LJLL laboratory to have a big, lively and benevolent community of PhD students, without which the time of my PhD would not have been as pleasant as it has been. I would like to thank for nice moments spent together : Amaury, Christophe, Jean, Jules, Rémi, Lise, Allen, Gontran and all the others and more particularly my officemates : Nicolas, Katia, Alexandre, Giorgia, Lucas, and Pierre as well as my French PhD brothers and sisters : Mathieu, Hugo and Cécile. Moreover, I am especially grateful towards Lilian and Idriss for some punctually life-saving help in Latex but also very nice and interesting discussions.
I also had the chance to get included in the very warm community of PhD students in Vienna, hence I would like to thank for nice moments spent together, some of my colleagues of the fourth floor namely Pietro, Axel, Paul, Giulia, Katharina, David, Melanie, Michael, Stefano, Elisa, Lara and Gaspard, but also some people of the Technical University of Vienna among which Anita, Max and Stefan as well as some members of the VDS/VSM of the third floor : Daniel, Giancarlo, and Christopher.
Among all the people I met during the PhD, I would like to give a very special thank to my wonderful PhD sister, Laura Kanzler, one of the rare persons that succeeds in being bright and kind at the same time, who has been a role model as well as a friend throughout my PhD.

I would like to thank my best friend Tom for our long passionate conversations and for accepting me as I am.

I dedicate this thesis to my mother, who has been supporting me since thirty years.

Accepter, s'agréger, être un rouage parmi d'autres rouages.

Roger Martin Du Gard, *Les Thibault*

Contents

Chapter 1

Introduction

Contents

1.1 A biological phenomenon : Autophagy

1.1.1 Presentation of selective autophagy

Autophagy, from the greek $\alpha\upsilon\tau o\varsigma$ (self) and $\varphi\alpha\gamma\varepsilon\iota\nu$ (to eat) is a process during which eukaryotic cells degrade unwanted or harmful intracellular substances and recycle their components. Together with the ubiquitin-proteasome system (UPS), autophagy constitutes one of the two major routes for the degradation of intracellular material. Several types of autophagy have been described but hereafter we will only consider macroautophagy, which will be referred to as autophagy. During autophagy, double membrane organelles called autophagosomes are created. Autophagosomes form from vesicular membrane precursors and grow as crescent-shaped membranes called isolation membranes. Isolation membranes engulf cytoplasmic material (cargo) until they seal into a closed double membrane vesicle, in which the cargo remains trapped. The autophagosomes then fuse with lysosomes, which contain enzymes able to degrade the autophagosomes' cargoes. These steps are recalled in Figure 1.1.

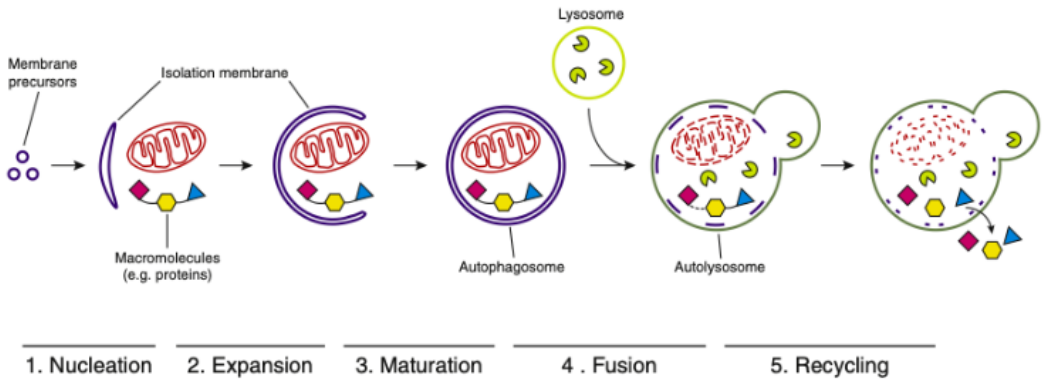

Figure 1.1: Autophagy delivers cytoplasmic material to the lysosomal compartment for degradation. (1) Membrane donors including Atg9 vesicles nucleate an isolation membrane. (2) The isolation membrane expands and engulfs cytoplasmic cargo material including organelles and macromolecules. (3) The isolation membrane matures into a closed double-membrane autophagosome. (4) The outer autophagosomal membrane fuses with a lysosome (or the vacuole in yeast), leading to the degradation of the inner membrane and the cargo. (5) Components are recycled back into the cytoplasm. This figure and the caption are taken from [64].

Autophagy is thought to be both non-selective and selective towards its cargoes. Non-selective autophagy happens during starvation and mainly serves to recycle building blocks, while selective autophagy degrades specific cargoes such as protein aggregates, damaged mitochondria, and intracellular pathogens. As a consequence, defects in autophagy have been associated with a wide range of diseases, such as neurodegeneration, cancer, and decreased innate immunity. For the rest of this dissertation only selective autophagy will be taken into account. Selective autophagic cargos are typically tagged with poly-ubiquitin (*i.e.* chains of ubiquitin molecules linked via different linkage types). Ubiquitinated cargos are then tethered to the isolation membranes by a cargo receptor protein. The most studied mammalian cargo receptor is p62/SQSTM1.

1.1.2 The cargo receptor p62/SQSTM1

The linking of the ubiquitinated cargo to the isolation membrane through p62/SQSTM1 is made possible thanks to two sites : the LIR motif, which is a binding site to molecules of the Atg8 family such as LC3B that are found attached to the membranes of autophagosomes, and the UBA domain, which is a binding site to Ubiquitin (See Figure 1.2). p62/SQSTM1 possess also a third site called PB1 domain that mediates self-oligomerization. To bind LC3B molecules, it is not enough for p62 to have a functional LIR motif domain (See [59]), it is also required that the PB1 oligomerization domain of p62 be functional, which means that the ability of p62 to bind cargoes depends on its ability to self-oligomerize. In addition to this role of cargo receptor, p62 has also been involved in the formation of ubiquitinated protein aggregates, which subsequently become cargos for autophagy (See [7] and [31]). This activity has been reconstituted in vitro in [65], which constitutes the object of the model presented in this dissertation. The capacity of p62 to self-oligomerize plays again an important role for the interaction between p62 and ubiquitin as discussed in further detail in 1.1.3.

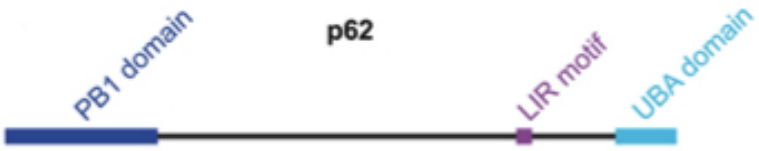

Figure 1.2: Schematic representation of the p62 domain architecture.

1.1.3 Interaction between p62/SQSTM1 and ubiquitin *in vitro*

The isolated UBA domain of p62 binds mono-ubiquitin with a relatively low affinity (According to [39], $K_d \approx 540\mu M$). Oligomers of p62 show a higher avidity with ubiquitin chains and in general with locally concentrated ubiquitin and, thus, stabilize the binding with the ubiquitinated cargo material (See [64]). However, the strength of this interaction depends also on the form of the ubiquitin with which oligomers of p62 binds. In [65], different forms of ubiquitin have been tested, among them ubiquitin chains but also mono-ubiquitin and multi-mono-ubiquitin. The conclusion of the study is that the interaction is the strongest (compared with mono-, bi-, tri-ubiquitin, and ubiqutin chains K48 and K63), when oligomers of p62 are in presence of tetra-ubiquitin.

1.2 First model

We designed a new model, which focuses on the interaction *in vitro* between oligomers of p62 and tetra-ubiquitin in the *in vitro* reconstitution of [65].

1.2.1 Modelling assumptions

We consider thus two types of basic particles:

1. *Oligomers* of the protein p62, where we assume for simplicity that all oligomers contain the same number $n \geq 3$ of molecules. These oligomers are denoted by p62_n and are assumed to possess n binding sites for ubiquitin each,

2. *Cross-linkers* in the form of tetra-ubiquitin, denoted by *Ubi* and assumed to have two ubiquitin ends each. When one end of a *Ubi* is bound to a p62_n, we call it *one-hand bound,* when both ends are bound we call it *both-hand bound.*

The modelling of the experiments [59] is quite complex and requires to consider aggregates formed from different particles. This corresponds also to a growing concern in Biology, as it is now clear that the heterogeneity of aggregates plays a major role in some phenomena such as the explanation of abnormal functionality in amyloid fibrils for instance (See [2]). To our knowledge, all the existing models in the literature consider aggregates described by one parameter, which is its unidimensional size (for polymers, it corresponds to the number of monomers it contains). For the majority of them, the aggregates are formed from one type of particle or species leading to a huge literature. Considering aggregates coming only from one species, has enabled to investigate a wide variety of phenomena : nucleation, polymerization (See [6]), depolymerization, fragmentation and coagulation (See [18], [3], [35]), although it does not describe the majority of the aggregates biologists and physicists face. This is why, reflecting the growing interest in Biology for taking into account the diversity of aggregates, very recent attempts (2018 for [17] and 2020 for [10]) have been made to take into account the plurality of monomers, such as in [17], where two types of monomers are considered, or as in [10]. Nevertheless, in the end, these attempts consider aggregates described by one

parameter, and thus fail to take into account the heterogeneity of real aggregates. When two types of particles are involved, which affects the structure of the aggregate as in our model, this is not anymore possible. It should be described at least by two parameters.
In our model, we decide to describe an aggregate by three parameters, in order to take into account the two different ways the two particles we are considering (Ubiquitin *one-hand bound* or *both-hand bound* to p62_n) could bind. Hence, in our model, an aggregate is represented by a triplet $(i, j, k) \in \mathbb{N}_0^3$, where :

1. i denotes the number of one-hand bound Ubi,
2. j denotes the number of both-hand bound Ubi,
3. k denotes the number of p62_n.

However, even by taking into account three parameters, our model fails to associate bijectively an aggregate with a triplet. In other words, as soon as $i, j, k > 1$, a same triplet represents several different aggregates.
In the first version of our model, we consider that :

1. aggregates grow in a medium with unlimited quantities of our two basic particles namely p62_n and Ubi
2. they do not interact with each other (no coagulation).

Thus we do not take into account in the first version of our model either coagulation or nucleation or fragmentation.

1.2.2 Model

To account for growth and shrinking of aggregates, we consider only three possible reactions that could be related to polymerization in some sense (adding of one of the two basic particles that play an equivalent role as the one played by monomers) and their reverse counterparts with associated (positive) kinetic reactions rates κ_1, κ_2, κ_3, κ_{-1}, κ_-, that are introduced in Chapter 2. This leads to an infinite discrete system similarly as the Becker-Döring system presented in [5] or as in [17], that we do not explicitely write because of the complexity brought by the three instead of one parameters describing one aggregate. We consider the growth of a population of aggregates of same size (i, j, k) with i, j, k large enough, so that they can be replaced by continuous parameters $p = \frac{i}{k_0}$, $q = \frac{j}{k_0}$ and $r = \frac{k}{k_0}$, with k_0 a typical value of $[Ubi]$ and $[p62n]$, assumed of the same order of magnitude. The system rewritten in terms of these continuous parameters is a transport equation (See Appendix A for the derivation). Finally, the equation satisfied by the characteristic curves of this transport equation is given by the following nonlinear ODE model :

$$\begin{aligned}
&\dot{p} = (\kappa_1 - \kappa_3 p)(nr - p - 2q) + \kappa_- q\left(1 - \frac{(n-1)p}{(n-2)r}\right) - (\kappa_2 + \kappa_{-1})p\,, && p(0) = p_0\,,\\
&\dot{q} = \kappa_2 p + \kappa_3 p(nr - p - 2q) - \kappa_- q\,, && q(0) = q_0\,,\\
&\dot{r} = \kappa_2 p - \kappa_- q\alpha(q, r)\,, && r(0) = r_0\,,
\end{aligned} \tag{1.1}$$

where

$$\alpha(q, r) := \frac{nr - 2q}{(n-2)r}, \quad 0 \le \alpha(q, r) \le 1, \quad nr - p - 2q \ge 0. \tag{1.2}$$

1.2.3 Analysis of the first model

We observe numerically three mutually exclusive regimes depending on the values of the parameters (the reactions rates κ_1, κ_2, κ_3, κ_{-1}, κ_-). We make the following conjecture :

Conjecture 1 (Chapter 2). *We define*

$$\bar{\alpha} = \frac{n}{n-2} + \frac{\kappa_{-1} + \kappa_1 - \sqrt{(\kappa_1 + \kappa_{-1})^2 + 4\kappa_1\kappa_2(n-1)}}{\kappa_-(n-1)}. \tag{1.3}$$

Then,

1. *if* $0 < \bar{\alpha} < 1$, *then all solutions of* (3.1) *converge to* $(\bar{p}, \bar{q}, \bar{r})$ *as* $t \to \infty$,
2. *if* $\bar{\alpha} \geq 1$, *then all solutions of* (3.1) *converge to* $(0, 0, 0)$ *as* $t \to \infty$,
3. *if* $\bar{\alpha} \leq 0$, *then for all solutions of* (3.1) *we have* $p(t), q(t), r(t) \to \infty$ *as* $t \to \infty$.

One can note that $\bar{\alpha}$ does not depend on the value of κ_3. Hence, it could seem that the different regimes do also not depend of the value of κ_3, which may question the relevance of the third reaction. In fact, the definition of the non-trivial steady-states $\bar{p}$, $\bar{q}$ and $\bar{r}$ as well as the expressions of p, q and r in the growing polynomial regime involve κ_3. The only necessary condition is that $\kappa_3 > 0$ (See Chapter 2). In the same chapter, we also study the case where $\kappa_3 = 0$ in which we do not observe these three regimes. The aim of the Chapter 3 is to prove partially this conjecture using dynamical systems tools, that we introduce hereafter in Subsection 1.3.1.

1.3 Dynamical systems tools used for the study of the first model

Basic notions of dynamical systems will not be recalled. The interested reader could have a look at [9], [46], [34] and [26].

In the Subsection 1.3.1, we recall the classical method to study of an ODE system, in order to show in the Subsection 1.3.2 that it does not apply to prove the Conjecture 1. In the Subsections 1.3.3 and 1.3.4, we introduce other dynamical system tools that enable us to prove partially the Conjecture 1 in the Chapter 3.

1.3.1 Classical study of the stability of the steady states of a non-linear ODE system

We consider the following general ODE system :

$$\dot{x} = f(x) \tag{1.4}$$

with $x \in \mathbb{R}^n$ is a vector and $f : \mathbb{R}^n \to \mathbb{R}^n$ a continuously differentiable function.

Definition. *A steady-state* $x_0 \in \mathbb{R}^n$ *is called hyperbolic, when all the eigenvalues of the Jacobian matrix at* x_0, *denoted hereafter* Df_{x_0}, *have their real part different from zero.*

Theorem (Hartman Grobman - quoted as in [9]). *If* x_0 *is a hyperbolic rest point for the autonomous differential equation* (1.4), *then there is an open set* U *containing* x_0 *and a homeomorphism* H *with domain* U *such that the orbits of the differential equation* (1.4) *are mapped by* H *to orbits of the linearized system* $\dot{x} = Df_{x_0}(x - x_0)$ *in the set* U.

1.3.2 Application to the ODE model

The ODE system (1.1) can be rewritten in the general form (1.4) with $n = 3$ and $x = (p, q, r)$. It admits two steady-states (See Section 2) :

1. the origin or zero steady-state $(p, q, r) = (0, 0, 0)$

2. a non-trivial steady-state $(\bar{p}, \bar{q}, \bar{r})$ given by :

$$\begin{aligned} \bar{p} &= \frac{\kappa_- \kappa_2}{\kappa_3} \frac{(n-(n-2)\bar{\alpha})(1-\bar{\alpha})}{2\bar{\alpha}(2\kappa_2(n-2)-\kappa_- n+\kappa_-(n-2)\bar{\alpha})}, \\ \bar{q} &= \frac{\kappa_2^2}{\kappa_3} \frac{(1-\bar{\alpha})}{\bar{\alpha}^2(2\kappa_2(n-2)-\kappa_- n+\kappa_-(n-2)\bar{\alpha})}, \\ \bar{r} &= 2\frac{\kappa_2^2}{\kappa_3} \frac{(1-\bar{\alpha})}{\bar{\alpha}^2(2\kappa_2(n-2)-\kappa_- n+\kappa_-(n-2)\bar{\alpha})}. \end{aligned} \tag{1.5}$$

1.3.2.1 Study of the zero steady-state

$\alpha(0,0)$ is not well-defined. Notwithstanding, the zero steady-state can still be defined because $\alpha(q,r)$ is bounded (see (1.2)), so that we have nevertheless that $q\alpha(q,r)$ is equal to 0 in $(q,r) = (0,0)$. However, the derivatives are not smooth. Consequently, the Jacobian matrix cannot be defined at the origin $(0,0,0)$. Thus, the stability of the zero steady-state $(0,0,0)$ cannot be studied using the methods mentioned in 1.3.1. To remove the singularity, we make the following time-change of variable $t \to \tau := \int_0^t \frac{\mathrm{d}s}{r(s)}$, which transforms the system (1.1) into the polynomial system (1.6), which is well-defined at $(p,q,r) = (0,0,0)$:

$$\begin{aligned} \frac{dp}{d\tau} &= (\kappa_1 - \kappa_3 p)(nr - p - 2q)r + \kappa_- q\left(r - \frac{(n-1)p}{(n-2)}\right) - (\kappa_2 + \kappa_{-1})pr\,, & p(0) &= p_0\,, \\ \frac{dq}{d\tau} &= \kappa_2 pr + \kappa_3 pr(nr - p - 2q) - \kappa_- q\,, & q(0) &= q_0\,, \\ \frac{dr}{d\tau} &= \kappa_2 pr - \kappa_- q(nr - 2q)\,, & r(0) &= r_0\,. \end{aligned} \tag{1.6}$$

The Jacobian matrix associated with (1.6) at $(0,0,0)$ is the zero matrix. Therefore, its three eigenvalues are zero, which makes $(0,0,0)$ a non-hyperbolic point for (1.6). Hence, the theory introduced in 1.3.1 cannot apply and we cannot study the stability with the classical theory the stability of the origin of our system. We introduce the blow-up theory that apply for non-hyperbolic points in the next subsection.

1.3.2.2 Study of the non-trivial steady-state

Before to studying the stability of the non-trivial steady-state, one should check its existence conditions. The formulae (1.5) are indeed not always defined. In Section 2, we show that they are well defined and positive when the quantity $\bar{\alpha}$ defined by (1.3) is between 0 and 1. When $\bar{\alpha} \in [0,1]$, one could theoretically compute the Jacobian matrix $Df_{(\bar{p},\bar{q},\bar{r})}$ and look at its eigenvalues. However, because of the formulae (1.5), this computation becomes intractable and not solvable even using computer tools such as Mathematica. Nevertheless, we conjecture in Section 2 from simulations of the system (1.1) that the non-trivial steady-state is stable for values of parameters κ_1, κ_2, κ_3, κ_{-1}, κ_-, such that $\bar{\alpha} \in [0,1]$.

1.3.3 Blow-up and application to the first model

To have a deeper understanding of blow-up, we refer to [26].

Blow-up enables to gain insight into what is happening in a neighbourhood of a non-hyperbolic point of a dynamical system. The idea is to blow up the non-hyperbolic point to a higher-dimensional structure such as a sphere, thanks to a change of variables that is not a diffeomorphism. The blow-up of a point into a sphere is called homogeneous blow-up. Although other forms are possible, we will not consider them as they are not necessary for the understanding of our case presented in Section 3. Then, one studies the singularities appearing on this new structure. If these new singularities are still non-hyperbolic, the procedure is repeated. We show hereafter the different steps of the blow-up of the origin of a vector field in $\mathbb{R}^3$ into a sphere $\mathbb{S}^2(\mathbb{R})$, similar as the one we do in Section 2.3. The

homogeneous blow-up (See Figure 1.3) $\Gamma : \mathbb{S}^2(\mathbb{R}) \times \mathbb{R}_+^* \to \mathbb{R}^3$ is a map that uses the same weights for each coordinate of the vector field :

$$\Gamma(\bar{p}, \bar{q}, \bar{r}, \rho) = (\rho\bar{p}, \rho\bar{q}, \rho\bar{r}) = (p, q, r).$$

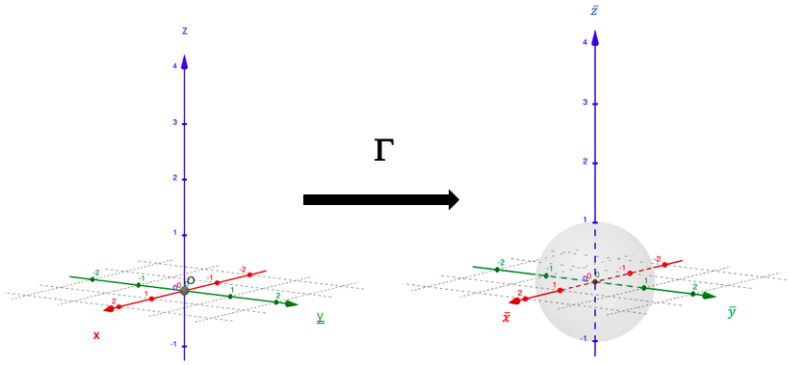

Figure 1.3: Blow-up of the origin $(0, 0, 0)$ into a sphere of radius ρ.

The dynamics in spherical coordinates is quite difficult to study. This is why often while not always suitable charts are chosen, where the computations of the blow-up are done in local coordinates. In $\mathbb{R}^3$, this defines the six following usual charts on the sphere $\mathbb{S}^2(\mathbb{R})$: $\mathcal{K}_p$ defined by $\mathcal{K}_p := \{(p, q, r) \in \mathbb{S}^2(\mathbb{R}) : p > 0\}$, $\mathcal{K}_q$ defined by $\mathcal{K}_q := \{(p, q, r) \in \mathbb{S}^2(\mathbb{R}) : q > 0\}$, $\mathcal{K}_r$ defined by $\mathcal{K}_r := \{(p, q, r) \in \mathbb{S}^2(\mathbb{R}) : r > 0\}$, $\mathcal{K}_{-p}$ defined by $\mathcal{K}_{-p} := \{(p, q, r) \in \mathbb{S}^2(\mathbb{R}) : p < 0\}$, $\mathcal{K}_{-q}$ defined by $\mathcal{K}_{-q} := \{(p, q, r) \in \mathbb{S}^2(\mathbb{R}) : q < 0\}$, and $\mathcal{K}_{-r}$ defined by $\mathcal{K}_{-r} := \{(p, q, r) \in \mathbb{S}^2(\mathbb{R}) : r < 0\}$. Only the three charts $\mathcal{K}_p$, $\mathcal{K}_q$ and $\mathcal{K}_r$ are necessary to describe the dynamics, when $p, q, r \geq 0$ as in Section 2.

Then, we have that for each $i = p, q, r, -p, -q, -r$, we have $\Gamma = \mathcal{K}_i \circ \mu_i$, where μ_i is the local blow-up map on $\mathcal{K}_i$. In each blow-up map, the dynamics is studied using the local coordinates. Typically, for the chart $\mathcal{K}_q$ used in Chapter 3, the local coordinates are $(p_1, q_1, r_1) = (pq, q, rq)$. Then, the dynamics of the local coordinates is computed from the original dynamics in each chart. In our case, because p,q and r are positive, we only have to consider the first positive octant of $\mathbb{S}^2(\mathbb{R})$. This means that we only have to consider the charts $\mathcal{K}_p$, $\mathcal{K}_q$, $\mathcal{K}_r$. Moreover, because of the two inequalities (1.2), the dynamics evolves only in a subset of this octant, where all the information could be provided by the chart $\mathcal{K}_q$. Studying the dynamics in the chart $\mathcal{K}_q$, we are able to prove the following theorem.

Theorem 5 (Chapter 3)**.** *Let $\bar{\alpha}$ be defined by (1.3). Then the steady state $(0, 0, 0)$ of the system (1.1) is locally asymptotically stable for $\bar{\alpha} > 1$ and unstable for $\bar{\alpha} < 1$.*

It proves partially the local stability of the trivial steady-state $(0, 0, 0)$ under the condition $\bar{\alpha} > 1$, which is a weakened version of the first conjecture of Conjecture 1. We now present the tools necessary to understand a proof of a weakened (also local) version of the third conjecture of Conjecture 1.

1.3.4 Poincaré-compactification, geometric singular perturbation theory and application to the first model

In fact, the third conjecture of Conjecture 1 can be refined using the following theorem (See Chapter 2).

Theorem 2 (Chapter 2)**.** *If $\bar{\alpha} < 0$, then there exists a formal approximation of a solution of (3.1) of the form*

$$p(t) = p_1 t + o(t)\,, \qquad q(t) = q_2 t^2 + o(t^2)\,, \qquad r(t) = \frac{2q_2}{n} t^2 + o(t^2)\,, \qquad \text{as } t \to \infty\,, \quad (1.7)$$

with

$$p_1 = \frac{\kappa_- n}{\kappa_3(2n\kappa_2+\kappa_- n+4\kappa_{-1})}\left(\kappa_1\kappa_2 - \frac{\kappa_- n}{2(n-2)}\left(\kappa_1 + \kappa_{-1} + \frac{\kappa_- n(n-1)}{2(n-2)}\right)\right) > 0\,,$$
$$q_2 = \frac{n}{2} r_2 = \frac{\kappa_3(n-2)(2n\kappa_2+\kappa_- n+4\kappa_{-1})}{\kappa_-(4\kappa_1(n-2)+\kappa_- n^2)} p_1^2\,.$$

The approximation is (from a formal point of view) unique, including the choice of the exponents of t, among solutions with polynomially or exponentially growing aggregate size r.

Hence, we can reformulate the third conjecture of Conjecture 1 by excluding the case $\bar{\alpha} = 0$ into the following :

Conjecture 2. *if $\bar{\alpha} < 0$, then all solutions converge towards infinity in the polynomial manner introduced in Theorem 2.*

In Chapter 3, we only prove a local result of this conjecture, which means that we have to look at $p(0)$, $q(0)$, and $r(0)$ close to infinity (actually, more detailed conditions expressing that $q(0)$ and $r(0)$ should be of the order of $p(0)^2$ are needed). To do so, we perform the change of variable $(p, q, r) \to (u = \frac{p}{\sqrt{p+q}}, v = \frac{2p+2q-nr}{\sqrt{p+q}}, w = \frac{1}{\sqrt{p+q}})$, which has been inspired by the Poincaré compactification that we explain hereafter.

1.3.4.1 Poincaré compactification

The Poincaré compactification allows to look at the behavior near infinity of a dynamical system. Basically, points $x \in \mathbb{R}^n$, with $n \geq 2$ are projected onto the sphere $\mathbb{S}^n$. The points $x \in \mathbb{R}^n$ that are near infinity, *i.e.* the points who have at least one of their coordinates x_i with $i \in [\![1, n]\!]$ close to infinity are projected onto the sphere $\mathbb{S}^{n-1}$ (See Figure 1.4). There is one projection in the upper-sphere $f^+(x)$ and one projection in the lower-sphere $f^-(x)$ (See Figure 1.4). Hereafter, we decided to present the theory for $n = 2$, which, we hope, will help the reader to better understand. The idea is to consider $\mathbb{R}^2$ as a plan in $\mathbb{R}^3$. A point (x_1, x_2) in $\mathbb{R}^2$ is thus bijectively associated to the point $(x_1, x_2, 1)$.

$$f^+(x) = \left(\frac{x_1}{\Delta(x)}, \frac{x_2}{\Delta(x)}, \frac{1}{\Delta(x)}\right)$$
$$f^-(x) = \left(\frac{-x_1}{\Delta(x)}, \frac{-x_2}{\Delta(x)}, \frac{-1}{\Delta(x)}\right) \quad (1.8)$$

with :

$$\Delta(x) = \sqrt{x_1^2 + x_2^2 + 1}.$$

This dynamics is quite complicated to study on $\mathbb{S}^2(\mathbb{R})$, this is why we consider it in the same local charts as in Blow-up (See Subsection 1.3.3). In the exact same way as in 1.3.3, the dynamics of the local coordinates can be rewritten and studied. Typically, in the chart $\mathcal{K}_1 = \{(x_1, x_2) \in \mathbb{S}^2(\mathbb{R}) : x_1 > 0\}$, the local coordinates are $(\frac{x_2}{x_1}, \frac{1}{x_1})$ (For more details, see [26]).

1.3.4.2 Application

In our case $p+q$ goes towards $+\infty$ and plays the role of the variable x_1, which goes towards $+\infty$ Hence, the variable w is equivalent to the variable $\frac{1}{x_1}$ and w goes to 0. Similarly, assuming that under the condition $\bar{\alpha} < 0$, the solutions converge towards the formal solution

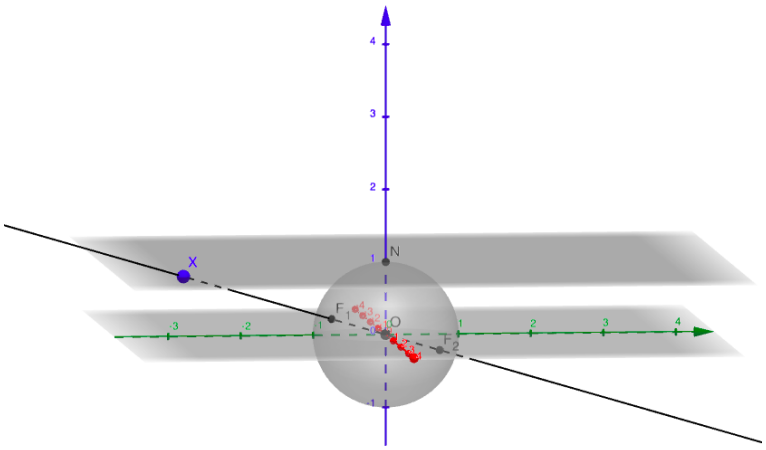

Figure 1.4: The point $x = (x_1, x_2)$ has two projections $F_1 := f^+(x)$ and $F_2 := f^-(x)$ defined by (A.2) on the sphere $\mathbb{S}^2(\mathbb{R})$. Points at infinity will be projected onto the circle which is the sphere $\mathbb{S}^1(\mathbb{R})$.

presented in Theorem 2, then u and v converge towards steady-states, similarly as the variable $\frac{x_2}{x_1}$ is also going towards a steady-state of the sphere $\mathbb{S}^1(\mathbb{R})$. Thus, we are able to translate the ODE for (p, q, r) into an ODE for (u, v, w). If we can prove locally that w goes like $\frac{1}{t^2}$ when t goes to infinity while u and v go towards steady-states when t goes to infinity, then we would have proven that (p, q, r) go towards infinity in the manner stated in Theorem 2. This is done in Chapter 3 using geometric singular perturbation theory, whose basic results are recalled in the following subsection.

1.3.4.3 Geometric singular perturbation theory

References for geometric singular perturbation theory are [34] and [11].

Now, we consider dynamical systems of the particular form :

$$\dot{x} = \varepsilon f(x, y, \varepsilon) \tag{1.9}$$
$$\dot{y} = g(x, y, \varepsilon) \tag{1.10}$$

where :

$$x \in \mathbb{R}^m, \quad y \in \mathbb{R}^n, \quad 0 < \varepsilon \ll 1, \quad f : \mathbb{R}^m \times \mathbb{R}^n \times \mathbb{R} \to \mathbb{R}^m, \quad g : \mathbb{R}^m \times \mathbb{R}^n \times \mathbb{R} \to \mathbb{R}^n.$$

x is called the slow variable and y the fast variable. Under the change of variable $\tau := \varepsilon t$, (1.9)-(1.10) becomes :

$$x' = f(x, y, \varepsilon) \tag{1.11}$$
$$\varepsilon y' = g(x, y, \varepsilon) \tag{1.12}$$

where $' := \frac{d}{d\tau}$. The system (1.11)-(1.12) (respectively (1.9)-(1.10)) is called the slow (respectively fast) system because the time τ is slower than the time t. When ε is equal to zero, on the one hand (1.9)-(1.10) becomes the system (1.13)-(1.14), which is called the layer problem. On the other hand, (1.11)-(1.12) becomes (1.15)-(1.16), which is called the reduced problem.

$$\dot{x} = 0 \tag{1.13}$$
$$\dot{y} = g(x, y, 0) \tag{1.14}$$

$$x' = f(x, y, 0) \tag{1.15}$$
$$0 = g(x, y, 0) \tag{1.16}$$

Now, we recall some definitions in order to quote the Fenichel's theorem which links the dynamics (1.9)-(1.10) and the dynamics (1.15)-(1.16) .

Definition. *The manifold C_0 defined by (1.16) is called the critical manifold, i.e. $C_0 = \{(x, y) \in \mathbb{R}^m \times \mathbb{R}^n : g(x, y, 0) = 0\}$.*

Definition (as in [34])**.** *A subset $S \subset C_0$ is called normally hyperbolic if the $n \times n$ matrix $(D_y g)(p, 0)$ of first partial derivatives with respect to the fast variables has no eigenvalues with zero real part for all $p \in S$.*

Definition. *A normally hyperbolic subset $S \subset C_0$ is called attracting if all eigenvalues of $(D_y g)(p, 0)$ have negative real parts for $p \in S$.*

Theorem (Fenichel - adapted and simplified from [34])**.** *Suppose $S = S_0$ is a compact normally hyperbolic submanifold (possibly with bound- ary) of the critical manifold C_0 of the slow system (1.11)-(1.12) and suppose that f, g smooth. Then for $\varepsilon > 0$ sufficiently small the following hold :*

1. *There exists a locally invariant manifold S_ε, diffeomorphic to S_0. Local invariance means that trajectories can enter or leave S_ε only through its boundaries.*
2. *S_ε is close to S_0.*
3. *The flow on S_ε converges to the slow flow as $\varepsilon \to 0$.*
4. *S_ε is normally hyperbolic and has the same stability properties with respect to the fast variables as S_0 (attracting, repelling or saddle-type).*

Applying this theorem twice in Chapter 3 enables us to prove the two following theorems.

Theorem 6 (Chapter 3)**.** *Let $\bar{\alpha} < 0$ hold. Then, for $\varepsilon > 0$ small enough, the solution of (3.12) with initial conditions*

$$u(0) = u_0 > 0\,, \qquad v(0) = v_0 \in \mathbb{R}\,, \qquad w(0) = \varepsilon\,,$$

satisfies

$$\begin{aligned} u(\tau) &= \hat{u}(\tau) - U(v_0) + U(\tilde{v}(\varepsilon\tau)) + O(\varepsilon)\,, \\ v(\tau) &= \tilde{v}(\varepsilon\tau) + O(\varepsilon)\,, \\ w(\tau) &= \varepsilon(1 + 2A^*\varepsilon^2\tau)^{-1/2} + O(\varepsilon^2)\,, \end{aligned}$$

uniformly in $\tau \geq 0$, where U, $\hat{u}$, $\tilde{v}$, and A^* are introduced in Chapter 3.

This theorem states that the variables u and v go towards steady-states and w goes towards 0 when $t \to \infty$, under the condition $\bar{\alpha} < 0$, which is exactly what we aimed at using the change of variable $(p, q, r) \to (u, v, w)$. This allows us to prove the last theorem which proves locally the third conjecture of Conjecture 1.

Theorem 7 (Chapter 3)**.** *Let $\bar{\alpha} < 0$ hold, let $c_2 \geq c_1 > 0$, and let $\delta > 0$ be small enough. Let the initial data satisfy*

$$p_0 = \frac{c_1}{\delta}\,, \qquad q_0 = \frac{1}{\delta^2}\,, \qquad r_0 = \frac{2}{n\delta^2} + \frac{c_2}{n\delta}$$

Then the solution of (3.1) with $(p(0), q(0), r(0)) = (p_0, q_0, r_0)$ satisfies

$$p(t) = u^* A^* t + o(t)\,, \qquad q(t) = (A^*)^2 t^2 + o(t^2)\,, \qquad r(t) = \frac{2}{n}(A^*)^2 t^2 + o(t^2)\,, \qquad \text{as } t \to \infty\,.$$

Hence, we have proven that under the condition $\bar{\alpha} < 0$, starting with initial conditions quoted as in Theorem 7, the solutions of (1.1) converge towards the formal solutions found in Theorem 2.

1.4 Improved model and perspectives

1.4.1 Adding coagulation

As explained in Chapter 4, it seems biologically relevant to take into account coagulation between aggregates in our model, which leads to unidimensional transport-coagulation or growth-coagulation equations, which have never been studied to our knowledge. The transport-coagulation equations that we study can be apparented to the following equation :

$$\begin{cases} \frac{\partial}{\partial t} f(x,t) + \frac{\partial}{\partial x}\big(v(x) f(x,t)\big) = & \frac{1}{2}\int_0^x k(x-y,y) f(x-y,t) f(y,t) dy \\ & - \int_0^\infty k(x,y) f(y,t) f(x,t) dy, \\ f(0,t) = f_0. \end{cases} \tag{1.17}$$

with $f_0 > 0$, $v(x)$ a C^1 decreasing function and $x_0 > 0$ such that $v(x_0) = 0$, $K(x,y)$ a symetric coagulation kernel - we shall consider here only $K(x,y) = 2$, $K(x,y) = x + y$ and $K(x,y) = xy$. In the following, we present properties of the classical continuous coagulation or Smoluchowski equation (See [54]) that will be useful for Chapter 4.

1.4.2 Continuous coagulation equations

Coagulation equations and its variant fragmentation-coagulation equations have been extensively studied in details these last years. Among many other, important references for coagulation equations are [1], [16] and for fragmentation-coagulation equations [18], [21], [4].

The continuous coagulation equation considers coagulation only between two particles and reads as follows :

$$\begin{aligned} &\partial_t f(x,t) = C(f,f) \\ &f(0,t) = f_0, \end{aligned} \tag{1.18}$$

with :

$$C(f,f) = C_1(f,f) - C_2(f,f) \tag{1.19}$$

$$C_1(f,f) = \frac{1}{2}\int_0^x k(x-y,y) f(x-y,t) f(y,t) dy \tag{1.20}$$

$$C_2(f,f) = f(x,t)\int_0^\infty k(x,y) f(y,t) dy. \tag{1.21}$$

k is the coagulation kernel, whose form is chosen depending on the physical experiment considered (See [50], [1]). C is the coagulation term. It can be divided in two terms $C_1(f,f)$ and $C_2(f,f)$, which expresses respectively how the system can gain (respectively lose) a particle of size x. A particle of size x is formed by coagulation between two particles of size $y \leq x$ and $x - y \geq 0$, while it is consumed by coagulation with particles of any size $y \geq 0$. The coagulation process decreases the number of particles and formally conserves the mass. Nevertheless, the conservation of mass can be violated at infinity when coagulation kernels are large enough (typically the multiplicative kernel $K(x,y) = xy$). This phenomenon is called gelation (See *e.g.* [21], [1], [16], [22]). Necessary and sufficient conditions to lead to gelation have been studied, especially, while adding other terms such as fragmentation, which is the opposite reaction of coagulation. Fragmentation counter-balances coagulation and a strong enough fragmentation kernel can prevent gelation (See [22]). Analogously, in Chapter 4, we proved for the multiplicative kernel that there exists a unique steady-state under certain assumptions on the transport term, which means that gelation can be prevented by a strong

enough transport term. Other phenomena have been extensively studied for coagulation and fragmentation-coagulation equations including self-similar solutions ([23]), stationary solutions ([36]) and convergence to equilibrium ([37]). We are especially interested in studying steady states that are biologically relevant. Steady-states have been previously studied for fragmentation-coagulation equations (See [19]). In Chapter 4, we find that transport-coagulation equations can admit exponential steady-states when prescribing very special transport speeds. Existence of steady-states for the multiplicative kernel is performed using a fix point theorem, inspired by [19]. We also studied Laplace transforms such as in [40] and [16], where the equations for the Laplace transforms (and desingularized Laplace transforms) and moments derived from the coagulation equation (1.19) are computed for the constant, additive and multiplicative kernels *i.e.* respectively $K(x, y) = 2$, $K(x, y) = x + y$, $K(x, y) = xy$. The equations derived for the desingularized Laplace transforms are particularly simple and allow to obtain information on the initial equation. Unfortunately, in the case of transport-coagulation equation, the equations derived from the Laplace transforms (or desingularized transforms) are far more complicated.

1.4.3 Perspectives

Perspectives of our work is an extensive study of the improved model both theoretically but also numerically in order to compare with biological data. Theoretically, we expect at short term to solve the moment problem presented in Chapter 4 and a convergence rate of the convergence toward the steady state obtained for the multiplicative kernel. At long term, we expect to have more general results and conditions on mass-conserving solutions and gelation for different types of kernels (not necessarily explicit). Numerically, we are currently working on a numerical scheme of a transport-coagulation equation inspired by [8], [29] and [25]. We expect to obtain simulations that could help us to make conjectures for the theoretical results but above all that could be compared to biological videos of G. Zaffagnini.
Other perspectives are adaptation of our model to other problems involving aggregates made out of two particles in biology.

Chapter 2

A mathematical model of p62-ubiquitin aggregates in autophagy

Contents

This chapter comes from an article that has been submitted to the Journal of Mathematical Biology *and has been written in collaboration with M. Doumic, S. Martens, C. Schmeiser and G. Zaffagnini.*

2.1 Introduction

Autophagy is an intracellular pathway, which targets damaged, surplus, and harmful cytoplasmic material for degradation. This is mediated by the sequestration of cytoplasmic cargo material within double membrane vesicles termed autophagosomes, which subsequently fuse with lysosomes wherein the cargo is hydrolyzed. Defects in autophagy result in various diseases including neurodegeneration, cancer, and uncontrolled infections [38]. The selectivity of autophagic processes is mediated by cargo receptors such as p62 (also known as SQSTM1), which link the cargo material to the nascent autophagosomal membrane [13]. p62 is an oligomeric protein and mediates the selective degradation of ubiquitinated proteins. Its interaction with ubiquitin is mediated by its C-terminal UBA domain, while it attaches the cargo to the autophagosomal membrane due to its interaction with Atg8 family proteins such as LC3B, which decorate the membrane [45]. Additionally, p62 serves to condensate ubiquitinated proteins into larger condensates or aggregates, which subsequently become targets for autophagy [55, 62]. It has been reported that this condensation reaction requires the ability of p62 to oligomerize and the presence of two or more ubiquitin chains on the substrates [59, 62].

In this chapter a mathematical model for the condensation process is derived and analyzed. It is based on cross-linking of p62 oligomers by ubiquitinated substrate [62]. A cross-linker is assumed to be able to connect two oligomers, where each oligomer has a number of binding sites corresponding to its size. As an approximation for the dynamics of large

aggregates, a nonlinear system of ordinary differential equations is derived.

The oligomerization property of p62 has been shown to be necessary in the formation of aggregates [62]: too small oligomers of Ubiquitin do not form aggregates [59].

The dynamics of protein aggregation has been studied by mathematical modelling for several decades, but most models consider the aggregation of only one type of protein, which gives rise to models belonging to the class of nucleation-coagulation-fragmentation equations, see e.g. [6,48,60] for examples in the biophysical literature, and [3,12,18,35] for a sample of the mathematical literature. Contrary to these studies, the present work considers aggregates composed of two different types of particles with varying mixing ratios, which drastically increases the complexity of the problem.

In the following section the mathematical model is derived. It describes an aggregate by three numbers: the number of p62 oligomers, the number of cross-linkers bound to one oligomer, and the number of cross-linkers bound to two oligomers. The model considers an early stage of the aggregation process where the supply of free p62 oligomers and of free cross-linkers is not limiting. Since no other information about the composition of the aggregate is used, assumptions on the binding and unbinding rates are necessary. In the limit of large aggregates, whose details are presented in an appendix, the model takes the form of a system of three ordinary differential equations. Section 3 starts with a result on the well posedness of the model, and it is mainly devoted to a study of the long-time behaviour by a combination of analytical and numerical methods. Depending on the parameter values, three different regimes are identified, where either aggregates are unstable and completely dissolved, or their size tends to a limiting value, or they keep growing (as long as they do not run out of free oligomers and cross-linkers). In Section 4 we discuss the parametrization of the model and a comparison with data from [62].

2.2 Presentation of the model

Discrete description of aggregates: We consider two types of basic particles:

1. *Oligomers* of the protein p62, where we assume for simplicity that all oligomers contain the same number $n \geq 3$ of molecules. These oligomers are denoted by $\mathrm{p62}_n$ and are assumed to possess n binding sites for ubiquitin each,

2. *Cross-linkers* in the form of ubiquitinated cargo, denoted by Ubi and assumed to have two ubiquitin ends each. When one end of a Ubi is bound to a $\mathrm{p62}_n$, we call it *one-hand bound,* when both ends are bound we call it *both-hand bound.*

An aggregate is represented by a triplet $(i, j, k) \in \mathbb{N}_0^3$, where i denotes the number of one-hand bound Ubi, j denotes the number of both-hand bound Ubi, and k denotes the number of $\mathrm{p62}_n$. It is a rather drastic step to describe an aggregate only by these three numbers, since the same triplet might represent aggregates with various forms. This will affect our modelling below.

An aggregate will be assumed to contain at least two $\mathrm{p62}_n$, i.e. $k \geq 2$, and enough both-hand bound Ubi to be connected, i.e. $j \geq k - 1$. Furthermore, an aggregate contains nk binding sites for Ubi, implying $i + 2j \leq nk$. A triplet $(i, j, k) \in \mathbb{N}_0^3$ satisfying the three inequalities

$$k \geq 2\,, \qquad j \geq k - 1\,, \qquad i + 2j \leq nk\,, \tag{2.1}$$

will be called *admissible.* An example of an admissible triplet describing a unique aggregate shape is $(0, k-1, k)$, representing a chain of $\mathrm{p62}_n$. Adding one both-hand bound Ubi already creates a shape ambiguity: The triplet $(0, k, k)$ can be realized by a circular aggregate or by an open chain, where one connection is doubled.

Figure 2.1: Examples for Reactions 1 (left) and 2 (right) with $\mathrm{p62}_5$ in black, one-hand bound Ubi in green, two-hand bound Ubi in red, free particles in blue. Reaction 1: $Ubi + (1,3,3) \to (2,3,3)$. Reaction 2: $\mathrm{p62}_5 + (2,3,3) \to (1,4,4)$.

The reaction scheme: Basically there are only two types of reactions: binding and unbinding of Ubi to $\mathrm{p62}_n$. However, depending on the situation these may have various effects on the aggregate, whence we distinguish between three binding and three unbinding reactions.

1. **Addition of a free** Ubi, requiring at least one free binding site, i.e. $nk - i - 2j \geq 1$, (see Fig. 2.1):

$$Ubi + (i,j,k) \xrightarrow{\kappa_1'} (i+1,j,k)$$

   The reaction rate (number of reactions per time) is modeled by mass action kinetics for a second-order reaction with reaction constant κ_1' and with the number $[Ubi]$ of free Ubi. Since free Ubi and free p62 oligomers will be assumed abundant, their numbers $[Ubi]$ and $[\mathrm{p62}_n]$ will be kept fixed and the abbreviation $\kappa_1 = \kappa_1'[Ubi]$ will be used. This leads to a first-order reaction rate

$$r_1 = \kappa_1(nk - i - 2j)\,. \tag{2.2}$$

2. **Addition of a free** $\mathrm{p62}_n$, requiring at least one one-hand bound Ubi, i.e. $i \geq 1$:

$$\mathrm{p62}_n + (i,j,k) \xrightarrow{\kappa_2'} (i-1,j+1,k+1)$$

   Analogously to above, we set $\kappa_2 = \kappa_2'[\mathrm{p62}_n]$ and

$$r_2 = \kappa_2 i\,. \tag{2.3}$$

3. **Compactification of the aggregate** by a Ubi binding its second hand, requiring at least one one-hand bound Ubi, i.e. $i \geq 1$, and at least one free binding site, i.e. $nk - i - 2j \geq 1$:

$$(i,j,k) \xrightarrow{\kappa_3'} (i-1,j+1,k)$$

   This is a second-order reaction with rate

$$r_3 = \kappa_3' i(nk - i - 2j)\,. \tag{2.4}$$

4. **Loss of a** Ubi, requiring at least one one-handed Ubi, i.e. $i \geq 1$. This is the reverse reaction to 1:

$$(i,j,k) \xrightarrow{\kappa_{-1}} Ubi + (i-1,j,k)$$

   Its rate is modeled by

$$r_{-1} = \kappa_{-1} i\,. \tag{2.5}$$

5. **Loss of a** $\mathrm{p62}_n$ (leading to loss of the whole aggregate if $k = 2$):

$$(i, j, k) \xrightarrow{\kappa_- \alpha_{j,k}} \mathrm{p62}_n + \ell\, Ubi + (i + 1 - \ell, j - 1, k - 1)$$

This and the following reaction need some comments. They are actually both the same reaction, namely breaking of a cross-link, which we assume to occur with rate $\kappa_- j$. However, this can have different consequences. Here we consider something close to the reverse of reaction 2. This means we assume that the broken cross-link has been the only connection of a p62 oligomer with the aggregate, such that the oligomer falls off. This requires the condition $nk - 2j \geq n - 1$, meaning the possibility that the other $n - 1$ binding sites of the lost oligomer are free of two-hand bound Ubi. It is not quite the reverse of reaction 2, since we have to consider the possibility that ℓ one-hand bound Ubi, $0 \leq \ell \leq n - 1$, are bound to the lost oligomer. The conditional probability $\alpha_{j,k}$ to be in this case, when a cross-link breaks, is *zero* for a very tightly connected aggregate where each oligomer is cross-linked at least twice, i.e. $nk - 2j \leq n - 2$, and it is *one* for a very loose aggregate, i.e. a chain with $j = k - 1$. This leads to the model

$$\alpha_{j,k} = \frac{(nk - 2j - n + 2)_+}{(n - 2)k + 4 - n}\,, \tag{2.6}$$

and to the rate

$$r_{-2} = \kappa_- \alpha_{j,k} j\,. \tag{2.7}$$

In the framework of our model, ℓ should be a random number satisfying the restrictions

$$(n - 1 - nk + i + 2j)_+ \leq \ell \leq \min\{i, n - 1\}\,, \tag{2.8}$$

where the upper bound should be obvious and the lower bound implies that the last condition in (2.1) is satisfied after the reaction. We shall use the choice

$$\ell = \ell_{i,j,k} := \left\lfloor \frac{(n - 1)i}{nk - 2j} \right\rceil\,, \tag{2.9}$$

which can be interpreted as the rounded ($\lfloor\cdot\rceil$ denotes the closest integer) expectation value for the number of one-hand bound Ubi on the lost oligomer in terms of the ratio between the number $n - 1$ of available binding sites on the lost oligomer and the total number $nk - 2j$ of available binding sites for one-hand bound Ubi in the whole aggregate. It is easily seen that in the relevant situation $\alpha_{j,k} > 0$, i.e. $nk - 2j \geq n - 1$, the choice (2.9) without the rounding satisfies the conditions (2.8). Since the bounds in (2.8) are integer, the same is true for the rounded version.

Note that we neglect the possibility to lose more than one oligomer by breaking a cross-link, i.e. the fragmentation of the aggregate into two smaller ones. This is a serious and actually questionable modelling assumption. An a posteriori justification will be provided by some of the results of the following section, showing that growing aggregates are tightly connected.

6. **Loosening of the aggregate** by breaking a cross-link, requiring at least one excess both-hand bound Ubi, i.e. $j \geq k$:

$$(i, j, k) \xrightarrow{\kappa_- (1 - \alpha_{j,k})} (i + 1, j - 1, k)\,.$$

This is the reverse of reaction 3 with the rate

$$r_{-3} = \kappa_- (1 - \alpha_{j,k}) j\,, \tag{2.10}$$

which respects the requirement $j \geq k$ for a positive rate, because of

$$1 - \alpha_{j,k} = \min\left\{1, \frac{2(j - k + 1)}{(n - 2)k + 4 - n}\right\}\,.$$

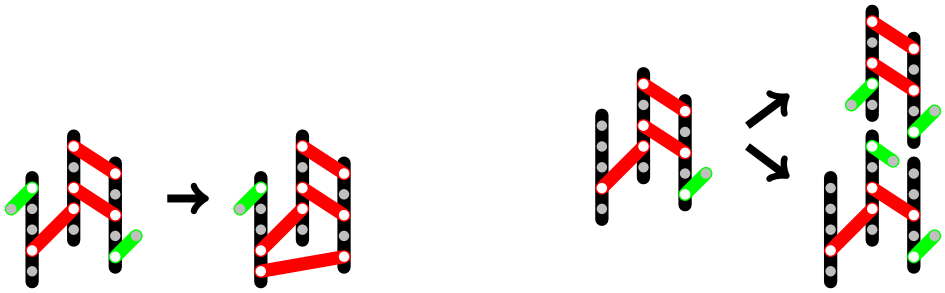

Figure 2.2: Examples for Reaction 3 (left, $(2,3,3) \to (1,4,3)$), Reaction 5 (right, up, $(1,3,3) \to \mathrm{p62}_5 + (2,2,2)$, $\ell = 0$), and Reaction 6 (right, down, $(1,3,3) \to (2,2,3)$).

A deterministic model for large aggregates: The next step is the formulation of an evolution problem for a probability density on the set of admissible states (i,j,k). In this problem the discrete state is scaled by a typical value k_0 of $[Ubi]$ and $[\mathrm{p62}_n]$, assumed of the same order of magnitude:

$$p := \frac{i}{k_0}\,, \qquad q := \frac{j}{k_0}\,, \qquad r := \frac{k}{k_0}\,. \tag{2.11}$$

It is then consistent with the definitions of κ_1 and κ_2 above to introduce $\kappa_3 := \kappa_3' k_0$. In the large aggregate limit $k_0 \to \infty$, the new unknowns become continuous, and the equation for the probability density becomes a transport equation (see Appendix A for the details). It possesses deterministic solutions governed by the ODE initial value problem

$$\begin{aligned}
&\dot p = (\kappa_1 - \kappa_3 p)(nr - p - 2q) + \kappa_- q\left(1 - \frac{(n-1)p}{(n-2)r}\right) - (\kappa_2 + \kappa_{-1})p\,, && p(0) = p_0\,,\\
&\dot q = \kappa_2 p + \kappa_3 p(nr - p - 2q) - \kappa_- q\,, && q(0) = q_0\,,\\
&\dot r = \kappa_2 p - \kappa_- q\alpha(q,r)\,, && r(0) = r_0\,,
\end{aligned} \tag{2.12}$$

where

$$\alpha(q,r) := \frac{nr - 2q}{(n-2)r} \tag{2.13}$$

is the limit of $\alpha_{j,k}$ as $k_0 \to \infty$. The conditions for admissible states $(p,q,r) \in [0,\infty)^2 \times (0,\infty)$ are obtained in the limit of (2.1):

$$s := nr - p - 2q \geq 0\,, \qquad q \geq r\,, \tag{2.14}$$

implying, as expected,

$$0 \leq \alpha(q,r) \leq 1\,. \tag{2.15}$$

The equations satisfied by s and $q - r$,

$$\dot s = (n-1)\kappa_2 p + \kappa_{-1} p + \kappa_- q\frac{2(q-r)}{(n-2)r} - s\left(\kappa_3 p + \kappa_1 + \kappa_- q\frac{n-1}{(n-2)r}\right), \tag{2.16}$$

$$(q-r)^{\cdot} = \kappa_3 p s - \frac{2\kappa_- q}{(n-2)r}(q-r)\,, \tag{2.17}$$

show that the conditions (2.14) are propagated by (3.1).

2.3 Analytic results

Global existence: Since the right hand sides of (3.1) contain quadratic nonlinearities, it seems possible that solutions blow up in finite time. On the other hand, the right hand sides

are not well defined for $r = 0$. The essence of the following global existence result is that neither of these difficulties occurs.

Theorem 1. *Let $3 \le n \in \mathbb{N}$ and $\kappa_1, \kappa_2, \kappa_3, \kappa_{-1}, \kappa_- \ge 0$. Let $(p_0, q_0, r_0) \in (0,\infty)^3$ satisfy (2.14). Then problem (3.1) has a unique global solution satisfying $(p(t), q(t), r(t)) \in (0,\infty)^3$ as well as (2.14) for any $t > 0$. Also the following estimates hold for $t > 0$:*

$$p(t) + q(t) + r(t) \le (p_0 + q_0 + r_0) \exp\left(t \max\{\kappa_1 n, \kappa_2\}\right), \tag{2.18}$$

$$r(t) \ge \frac{2}{n} q(t) \ge \frac{2q_0}{n} \exp(-\kappa_- t). \tag{2.19}$$

Proof. Local existence and uniqueness is a consequence of the Picard-Lindelöf theorem. Global existence will follow from the bounds stated in the theorem. Positivity of the solution components, of $s = nr - p - 2q$, and of $q - r$ is an immediate consequence of the form of the equations (3.1), (2.16), (2.17). This also implies

$$\dot{p} + \dot{q} + \dot{r} \le \kappa_1 nr + \kappa_2 p \le \max\{\kappa_1 n, \kappa_2\}(p + q + r),$$

which shows (2.18) by the Gronwall lemma. With (2.14), the equation for q in (3.1) implies

$$\dot{q} \ge -\kappa_- q,$$

and another application of the Gronwall lemma and of (2.14) proves (2.19) and, thus, completes the proof of the theorem. □

Long-time behaviour: The first step in the long-time analysis is the investigation of steady states. Although the right hand sides of (3.1) are not well defined for $r = 0$, the origin $p = q = r = 0$ can be considered as a steady state since

$$0 \le \alpha(q, r) \le 1 \qquad \text{and} \qquad \frac{p}{r} \le n$$

hold for admissible states satisfying (2.14). The origin is the only acceptable steady state with $r = 0$, since $\alpha(q, r)$ and p/r are not well defined in this case, so the factor q, multiplying them in the equations, needs to be zero. Finally, for a steady state this implies also $p = 0$. The following result shows that at most one other steady state is possible which, somewhat miraculously, can be computed explicitly.

Theorem 2. *Let $3 \le n \in \mathbb{N}$, $\kappa_1, \kappa_2, \kappa_3, \kappa_{-1}, \kappa_- > 0$, and let*

$$\bar{\alpha} := \frac{n}{n-2} + \frac{\kappa_{-1} + \kappa_1 - \sqrt{(\kappa_1 + \kappa_{-1})^2 + 4\kappa_1\kappa_2(n-1)}}{\kappa_-(n-1)} \tag{2.20}$$

satisfy $0 < \bar{\alpha} < 1$. Then there exists an admissible steady state $(\bar{p}, \bar{q}, \bar{r}) \in (0,\infty)^3$ of (3.1) given by

$$\begin{aligned}
\bar{p} &= \frac{\kappa_1\kappa_2(n-2)}{\kappa_3(\kappa_-\hat{q}(n-1) + \kappa_{-1}(n-2))} \frac{1-\bar{\alpha}}{\bar{\alpha}}, \\
\bar{q} &= \frac{\kappa_1\kappa_2^2(n-2)}{\kappa_3\kappa_-(\kappa_-\hat{q}(n-1) + \kappa_{-1}(n-2))} \frac{1-\bar{\alpha}}{\bar{\alpha}^2}, \\
\bar{r} &= \frac{\kappa_1\kappa_2^2(n-2)}{\hat{q}\kappa_3\kappa_-(\kappa_-\hat{q}(n-1) + \kappa_{-1}(n-2))} \frac{1-\bar{\alpha}}{\bar{\alpha}^2},
\end{aligned}$$

with $\bar{\alpha} = \alpha(\bar{q}, \bar{r})$ and $\hat{q} = (n - (n-2)\bar{\alpha})/2 \in (1, n/2)$. There exists no other steady state (besides the origin).

Proof. Assuming $\bar{r} > 0$, we introduce

$$\hat{p} = \frac{\bar{p}}{\bar{r}}\,, \qquad \hat{q} = \frac{\bar{q}}{\bar{r}}\,, \tag{2.21}$$

and rewrite the steady state equations in terms of $\hat{p}$ and $\hat{q}$:

$$0 = (\kappa_1 - \kappa_3\bar{p})(n - \hat{p} - 2\hat{q}) + \kappa_-\hat{q}\left(1 - \hat{p}\frac{n-1}{n-2}\right) - (\kappa_2 + \kappa_{-1})\hat{p}\,, \tag{2.22}$$

$$0 = \kappa_2\hat{p} + \kappa_3\bar{p}(n - \hat{p} - 2\hat{q}) - \kappa_-\hat{q}\,, \tag{2.23}$$

$$0 = \kappa_2\hat{p} - \kappa_-\hat{q}\bar{\alpha}\,, \qquad \text{with } \bar{\alpha} = \frac{n-2\hat{q}}{n-2}\,. \tag{2.24}$$

From (2.24) we obtain

$$\hat{p} = \frac{\kappa_-\hat{q}}{\kappa_2}\bar{\alpha} = \frac{\kappa_-\hat{q}(n-2\hat{q})}{\kappa_2(n-2)}\,, \tag{2.25}$$

which is substituted into the sum of (2.22) and (2.23):

$$(n-2\hat{q})\left(\kappa_1 - \frac{\kappa_1\kappa_-}{\kappa_2(n-2)}\hat{q} - \frac{\kappa_-^2(n-1)}{\kappa_2(n-2)^2}\hat{q}^2 - \frac{\kappa_{-1}\kappa_-}{\kappa_2(n-2)}\hat{q}\right) = 0\,.$$

The option $n = 2\hat{q}$ leads to $\bar{\alpha} = 0$, implying $\hat{p} = 0$ and, thus, $\bar{p} = 0$, which contradicts (2.23). Therefore the second paranthesis has to vanish, leading to a quadratic equation for $\hat{q}$ with the only positive solution

$$\hat{q} = \frac{(n-2)\left(-\kappa_{-1} - \kappa_1 + \sqrt{(\kappa_1+\kappa_{-1})^2 + 4\kappa_1\kappa_2(n-1)}\right)}{2\kappa_-(n-1)}\,.$$

Now (2.24) implies the formula for $\bar{\alpha}$ stated in the theorem and we note that $0 < \bar{\alpha} < 1$ implies $1 < \hat{q} < n/2$. We compute $\hat{p}$ from $\hat{q}$ by (2.25) and note that $\hat{p} > 0$ since $\bar{\alpha} > 0$. We then compute $\hat{s} = \bar{s}/\bar{r} = n - \hat{p} - 2\hat{q}$ from the sum of (2.22) and (2.23):

$$\hat{s} = \hat{p}\frac{\kappa_{-1}(n-2) + \kappa_-\hat{q}(n-1)}{(n-2)\kappa_1} = \frac{\kappa_-\hat{q}\,(\kappa_{-1}(n-2) + \kappa_-\hat{q}(n-1))}{(n-2)\kappa_1\kappa_2}\bar{\alpha}\,,$$

which proves $\hat{s} > 0$. Finally we obtain the formula for $\bar{p}$ from (2.23) as well as $\bar{r} = \bar{p}/\hat{p}$ and $\bar{q} = \bar{r}\hat{q}$. □

For convenience below, the conditions in the theorem are made more explicit in terms of the parameters by

$$\bar{\alpha} < 1 \quad\Leftrightarrow\quad \hat{q} > 1 \quad\Leftrightarrow\quad \kappa_1\kappa_2 > \frac{\kappa_-}{n-2}\left(\kappa_1 + \frac{n-1}{n-2}\kappa_- + \kappa_{-1}\right)\,, \tag{2.26}$$

$$\bar{\alpha} > 0 \quad\Leftrightarrow\quad \hat{q} < \frac{n}{2} \quad\Leftrightarrow\quad \kappa_1\kappa_2 < \frac{\kappa_- n}{2(n-2)}\left(\kappa_1 + \frac{n(n-1)}{2(n-2)}\kappa_- + \kappa_{-1}\right)\,. \tag{2.27}$$

The steady state approaches the origin $p = q = r = 0$ as $\bar{\alpha} \to 1$, whereas all its components become unbounded as $\bar{\alpha} \to 0$. This motivates the following.

Conjecture 1. *With the notation of Theorem 2,*

1. *if $0 < \bar{\alpha} < 1$, then all solutions of (3.1) converge to $(\bar{p}, \bar{q}, \bar{r})$ as $t \to \infty$,*
2. *if $\bar{\alpha} \geq 1$, then all solutions of (3.1) converge to $(0, 0, 0)$ as $t \to \infty$,*
3. *if $\bar{\alpha} \leq 0$, then for all solutions of (3.1) we have $p(t), q(t), r(t) \to \infty$ as $t \to \infty$.*

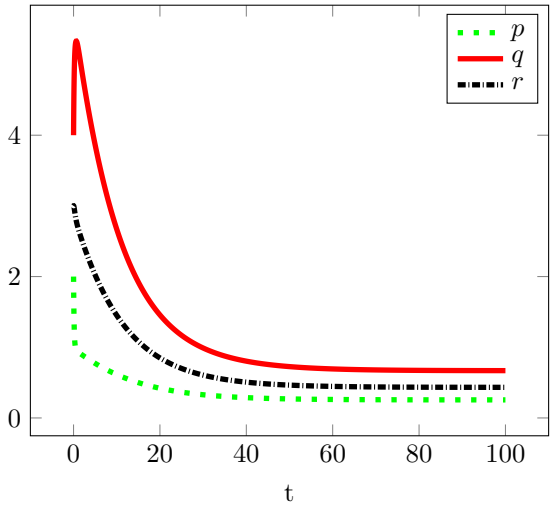

Figure 2.3: Convergence to the non-trivial steady state of Theorem 2. Simulation of an aggregate (p, q, r) of initial size $(2, 4, 3)$ with parameters $\kappa_1 = \kappa_2 = \kappa_3 = \kappa_{-1} = 1$ and $\kappa_- = 0.6$, implying $0 < \bar{\alpha} < 1$.

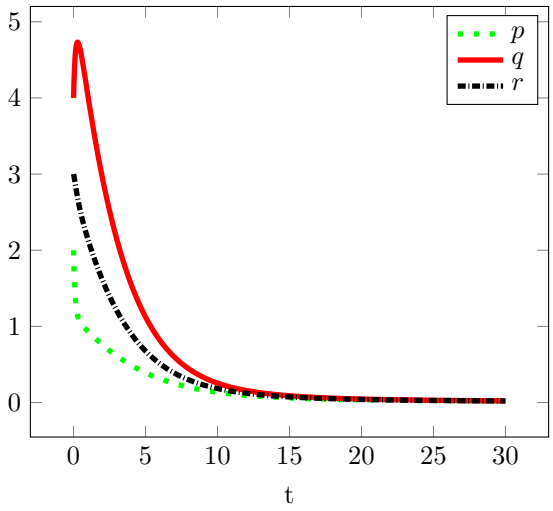

Figure 2.4: Instability of the aggregate. Simulation of an aggregate (p, q, r) of initial size $(2, 4, 3)$ with parameters $\kappa_1 = \kappa_2 = \kappa_3 = \kappa_{-1} = 1$ and $\kappa_- = 0.93$, implying $\bar{\alpha} > 1$.

The conjecture has been supported by numerical simulations. Figures 2.3, 2.4, and 2.5 show typical simulation results corresponding to the three cases. The conjecture is open, and its proof is not expected to be easy. Note for example that not even the local stability of the origin in Case 2 can be investigated by standard methods, since the right hand side of (3.1) lacks sufficient smoothness. Partial results will be published in separate work.

Closer inspection of the simulation results for growing aggregates (see Figure 2.5) shows that the growth is polynomial in time. This is verified by the following formal result.

Theorem 3. *With the notation of Theorem 2, if $\bar{\alpha} < 0$, then there exists a formal approximation of a solution of (3.1) of the form*

$$p(t) = p_1 t + o(t)\,, \qquad q(t) = q_2 t^2 + o(t^2)\,, \qquad r(t) = r_2 t^2 + o(t^2)\,, \qquad \text{as } t \to \infty\,, \quad (2.28)$$

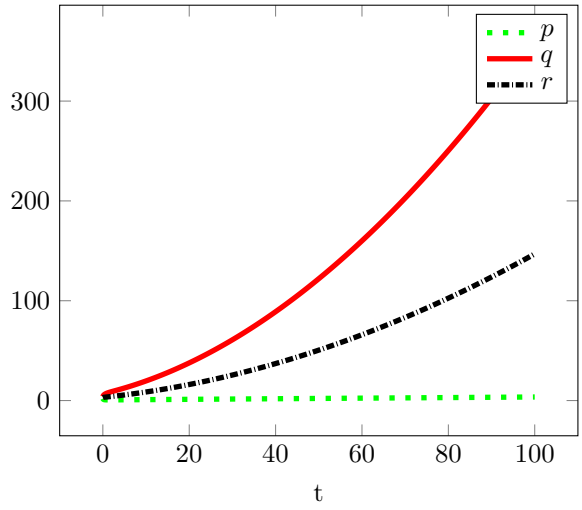

Figure 2.5: Growth of the aggregate. Simulation of an aggregate (p, q, r) of initial size $(2, 4, 3)$ with parameters $\kappa_1 = \kappa_2 = \kappa_3 = \kappa_{-1} = 1$ and $\kappa_- = 0.2$, implying $\bar{\alpha} < 0$.

with

$$\begin{aligned} p_1 &= \tfrac{\kappa_- n}{\kappa_3(2n\kappa_2+\kappa_- n+4\kappa_{-1})}\left(\kappa_1\kappa_2 - \tfrac{\kappa_- n}{2(n-2)}\left(\kappa_1 + \kappa_{-1} + \tfrac{\kappa_- n(n-1)}{2(n-2)}\right)\right) > 0\,, \\ q_2 &= \tfrac{n}{2} r_2 = \tfrac{\kappa_3(n-2)(2n\kappa_2+\kappa_- n+4\kappa_{-1})}{\kappa_-(4\kappa_1(n-2)+\kappa_- n^2)} p_1^2\,. \end{aligned} \tag{2.29}$$

The approximation is (from a formal point of view) unique, including the choice of the exponents of t, among solutions with polynomially or exponentially growing aggregate size r.

Proof. Since $2r \le 2q \le nr$ holds for admissible states, when $r(t)$ tends to infinity, then also $q(t)$ tends to infinity at the same rate, which we write with the *sharp order symbol* O_s as

$$q(t) = O_s(r(t)) \qquad \text{as } t \to \infty\,. \tag{2.30}$$

With $\alpha = \frac{s+p}{(n-2)r}$, we write the equations for r and for $p + q$ as

$$\dot{r} = \kappa_2 p - (s+p)\frac{\kappa_- q}{(n-2)r}\,, \qquad \dot{p} + \dot{q} = \kappa_1 s - p\left(\frac{\kappa_-(n-1)q}{(n-2)r} + \kappa_{-1}\right)\,. \tag{2.31}$$

Since the right hand sides have to be asymptotically nonnegative by the growth of q and r, taking (2.30) into account, the first equation implies $s(t) = O(p(t))$, and the second implies $p(t) = O(s(t))$, i.e.

$$s(t) = O_s(p(t)) \qquad \text{as } t \to \infty\,. \tag{2.32}$$

If the growth were exponential, i.e. $r(t), q(t) = O_s(e^{\lambda t})$, $\lambda > 0$, then (2.31) would imply $p(t), s(t) = O_s(e^{\lambda t})$. Then the negative term $-\kappa_3 p(t)s(t) = O_s(e^{2\lambda t})$ in the first equation in (3.1) could not be balanced by any of the positive terms, and would drive p to negative values. This contradiction excludes exponential growth.

For polynomial growth, i.e. $r(t), q(t) = O_s(t^\gamma)$, (2.31) implies $p(t), s(t) = O_s(t^{\gamma-1})$. In the equation for q in (3.1), $\dot{q}$ and p are small compared to q. Therefore it is necessary that $s(t)p(t) = O_s(q(t))$, implying $2\gamma - 2 = \gamma$ and, thus, $\gamma = 2$. This justifies the ansatz (2.28) with the addition $s(t) = s_1 t + o(t)$. Substitution into the differential equations and

comparison of the leading-order terms gives equations for the coefficients:

$$\begin{aligned}
\text{2nd equ. in (3.1):} \qquad & 0 = \kappa_3 p_1 s_1 - \kappa_- q_2 \,, \\
\text{(2.17):} \qquad & 0 = \kappa_3 p_1 s_1 - \kappa_- q_2 \,(1 - \alpha(q_2, r_2)) \,, \\
\text{1st equ. in (2.31):} \qquad & 2r_2 = \kappa_2 p_1 - (s_1 + p_1) \frac{\kappa_- q_2}{(n-2) r_2} \,, \\
\text{2nd equ. in (2.31):} \qquad & 2q_2 = \kappa_1 s_1 - p_1 \left(\frac{\kappa_-(n-1) q_2}{(n-2) r_2} + \kappa_{-1} \right) \,,
\end{aligned}$$

This system can be solved explicitly by first noting that the first two equations imply $\alpha(q_2, r_2) = 0$ and, thus, $2q_2 = nr_2$. Using this in the third and fourth equation gives a linear relation between p_1 and s_1. This again can be used in the fourth equation to write q_2 as a linear function of s_1. The division of the first equation by s_1 then gives the formula for p_1 in (2.29). The positivity of p_1 is a consequence of (2.27). □

For all the results so far the positivity of the rate constant κ_- for breaking cross-links has been essential. Therefore it seems interesting to consider the special case $\kappa_- = 0$ separately. It turns out that the dynamics is much simpler. The aggregate size always grows linearly with time.

Theorem 4. *Let $3 \le n \in \mathbb{N}$, $\kappa_1, \kappa_2, \kappa_3, \kappa_{-1} > 0$, and $\kappa_- = 0$. Let $(p_0, q_0, r_0) \in (0, \infty)^3$ satisfy (2.14). Then the solution of (3.1) satisfies*

$$\lim_{t\to\infty} p(t) = p_\infty := \frac{(n-2)\kappa_1\kappa_2}{\kappa_3(\kappa_2(n-2) + \kappa_{-1})} \,, \qquad \lim_{t\to\infty} s(t) = s_\infty := \frac{(n-2)\kappa_2}{2\kappa_3} \,,$$

$$q(t) = p_\infty(\kappa_2 + \kappa_3 s_\infty)t + o(t) \,, \qquad r(t) = \kappa_2 p_\infty t + o(t) \,, \qquad \text{as } t \to \infty \,.$$

Proof. For $\kappa_- = 0$ the right hand sides in (3.1) depend only on p and $s = nr - 2q - p$, meaning that these two variables solve a closed system:

$$\begin{aligned}
\dot p &= \kappa_1 s - (\kappa_2 + \kappa_{-1} + \kappa_3 s) p \,, \\
\dot s &= ((n-1)\kappa_2 + \kappa_{-1}) p - (\kappa_1 + \kappa_3 p) s \,.
\end{aligned}$$

The unique nontrivial steady state (p_∞, s_∞) can be computed explicitly. We prove that it is globally attracting by constructing a Lyapunov functional. Let $a \ge 1$ and

$$R_a := \left[\frac{p_\infty}{a}, a p_\infty \right] \times \left[\frac{s_\infty}{a}, a s_\infty \right] \,.$$

For each point $(p, s) \in (0, \infty)^2$ there is a unique value of $a \ge 1$ such that $(p, s) \in \partial R_a$. Therefore the Lyapunov function

$$L(p, s) := a - 1 \qquad \text{for } (p, s) \in \partial R_a \,,$$

is well defined and definite in the sense $L(p, s) \ge 0$ with equality only for $(p, s) = (p_\infty, s_\infty)$. It remains to prove that the flow on ∂R_a is strictly inwards. For example, for the left boundary part,

$$\dot p \,\big|_{(p,s)\in\{p_\infty/a\}\times[s_\infty/a, a s_\infty]} > \left(\kappa_1 - \kappa_3 \frac{p_\infty}{a} \right) \frac{s_\infty}{a} - (\kappa_2 + \kappa_{-1}) \frac{p_\infty}{a} = \frac{\kappa_3 p_\infty s_\infty (a-1)}{a^2} > 0 \,,$$

where for the first inequality it has been used that $p_\infty < \kappa_1/\kappa_3$, and the equality follows from the fact that $\dot p$ vanishes at the steady state. Similarly it can be shown that $\dot p < 0$ on the right boundary part, $\dot s > 0$ on the lower boundary part, and $\dot s < 0$ on the upper boundary part.

The linear growth of q and r follows from

$$\lim_{t\to\infty} \dot q(t) = \kappa_2 p_\infty + \kappa_3 p_\infty s_\infty \,, \qquad \lim_{t\to\infty} \dot r(t) = \kappa_2 p_\infty \,.$$

□

This result shows that the breakage of cross-links has somewhat contradictory effects, depending on the parameter regime: It can speed-up the aggregation dynamics, producing a quadratic rather than linear growth of the aggregate size (Case 3 of Conjecture 1). This is linked to the fact that it allows the aggregates to rearrange in a more compact way. On the other hand, it may slow down the dynamics, such that the aggregate only reaches a finite size (Case 1) or even disintegrates completely (Case 2).

2.4 Comparison with experimental data — Discussion

Comparison with experimental data: There are only limited options for a serious comparison of the theoretical results with experimental data. We shall use the data shown in Figure 2.6, which have been published in [62]. It provides observed numbers of aggregates in dependence of ubiquitin for a fixed concentration of p62. Our results do not permit a direct comparison with this curve, which would require modelling of the process of nucleation of aggregates. However, the data provide at least some information about concentration levels of ubiquitin and p62, such that stable aggregates exist.

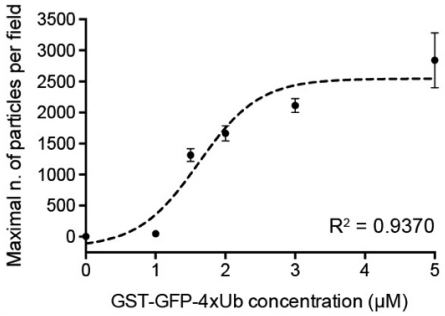

Figure 2.6: Number of aggregates in terms of $[Ubi]$ (or more precisely $(4 \times Ubi - GST - GFP)_2$) at fixed [p62]= $2\mu M$ [62]. Average and SD among three independent replicates are shown. The dashed line represents a fitted sigmoidal (more precisely, logistic) function, centered around $[Ubi] = 1.6\mu M$. Note that here p62 monomers are counted. Under the assumption that p62 only occurs in oligomers of size n we have [p62]=n[p62$_n$]. The regression coefficient R^2 measures the quality of the fit.

For meaningful quantitative comparisons with these scarce data we need to reduce the number of parameters in our model. As a first step, we fix the value $n = 5$ of the size of p62 oligomers, following [62] where values between 5 and 6 for GFP-p62 have been found (although we note that in [59] an average of about $n = 24$ has been reported for mCherry-p62 in vitro). This implies that the experiment corresponds to an oligomer concentration of $[\text{p62}_5] = [p62]/5 = 0.4\mu M$.

Concerning the rate constants, we make the assumption that the binding and, respectively, the unbinding rate constants are equal, i.e. $\kappa_1' = \kappa_2' = \kappa_3'$ and $\kappa_{-1} = \kappa_-$. This will allow to express all our results in terms of one *dissociation constant* $K_d := \kappa_{-1}/\kappa_1'$.

From Figure 2.6 we conclude that for an oligomer concentration of $[\text{p62}_5] = 0.4\mu M$ the growth of stable aggregates requires a cross-linker concentration $[Ubi]$ roughly between $0.6\mu M$ and $2.6\mu M$ ($(1.6 \pm 1)\mu M$). According to the results of the preceding section, these values should correspond to situations with either $\bar{\alpha} = 0$ or $\bar{\alpha} = 1$, depending on the question, if the equilibrium aggregate sizes of Case 1 in Conjecture 1 are large enough to be detected in the experiment, or if we need to be in Case 3 of growing aggregates. Therefore, with the

above assumptions, with $\kappa_1 = \kappa_1'[Ubi]$, $\kappa_2 = \kappa_2'[\mathrm{p62}_5]$, and with (2.26), (2.27), we obtain for $\bar{\alpha} = 1$:

$$[\mathrm{p62}_n]\,[Ubi] = \frac{K_d}{n-2}\left([Ubi] + \frac{(2n-3)K_d}{n-2}\right), \tag{2.33}$$

and for $\bar{\alpha} = 0$:

$$[\mathrm{p62}_n]\,[Ubi] = \frac{nK_d}{2(n-2)}\left([Ubi] + \frac{(n^2+n-4)K_d}{2(n-2)}\right). \tag{2.34}$$

Solving these equations for K_d with $n = 5$, $[\mathrm{p62}_n] = 0.4\mu M$, and with $[Ubi]$ between $0.6\mu M$ and $2.6\mu M$, gives estimates for K_d between $0.44\mu M$ and $0.73\mu M$ for $\bar{\alpha} = 1$, and between $0.20\mu M$ and $0.31\mu M$ for $\bar{\alpha} = 0$. So we claim that at least the order of magnitude is significant. It differs by three orders of magnitude from published data on the reaction between ubiquitin and the UBA domain of p62 ($K_d \approx 540\mu M$ [39]). This should not be so surprising, since in the context of growing aggregates the reactions can be strongly influenced by avidity effects.

Discussion: We return to Conjecture 1, where the long-time behaviour is described in terms of the value of the parameter $\bar{\alpha}$ defined in (2.20). With the simplifying assumptions on the reaction rate constants from above, the statements of the conjecture are depicted in Figure 2.7 for the fixed values $n = 5$ and $K_d = 0.5\mu M$ (motivated by the estimates above) in a bifurcation diagram in terms of the concentrations $[Ubi]$ and $[\mathrm{p62}_n]$. Note the unsymmetry in the dependence on the two quantities: The critical values for $[Ubi]$ tend to zero as $[\mathrm{p62}_n]$ tends to infinity, whereas the critical values for $[\mathrm{p62}_n]$ tend to the positive values $\frac{K_d}{n-2}$ for $\bar{\alpha} = 1$ and $\frac{nK_d}{2(n-2)}$ for $\bar{\alpha} = 0$, as $[Ubi]$ tends to infinity.

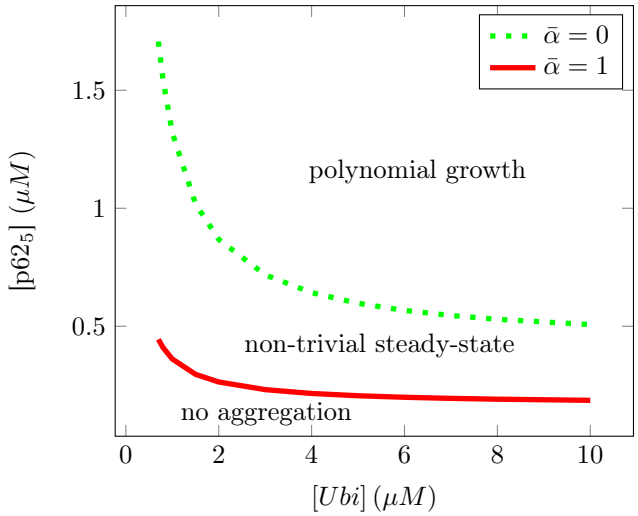

Figure 2.7: Bifurcation diagram corresponding to Conjecture 1 for $n = 5$, $K_d = 0.5\mu M$.

There is a significant uncertainty concerning the oligomer size n, which has so far been assumed to be 5, according to observations in [62]. Actually, a distribution of oligomer sizes should be expected in the experiments of Figure 2.6 with the occurrence of much larger oligomers. For this reason the computation of K_d from (2.33) has been repeated for a range of values of n between $n = 3$ and $n = 100$. The results are depicted in Figure 2.8, which shows that the predicted values of K_d might be larger by up to an order of magnitude compared to the case $n = 5$, but still small compared to [39], if larger oligomer sizes are considered and $\bar{\alpha} = 1$ is relevant. The asymptotic behaviour for large oligomer sizes is easily seen to be $K_d = O(n^{1/2})$. On the other hand, if $\bar{\alpha} = 0$ is relevant, the value of K_d becomes

smaller by up to an order of magnitude for large oligomers with the asymptotic behaviour $K_d = O(n^{-1/2})$.

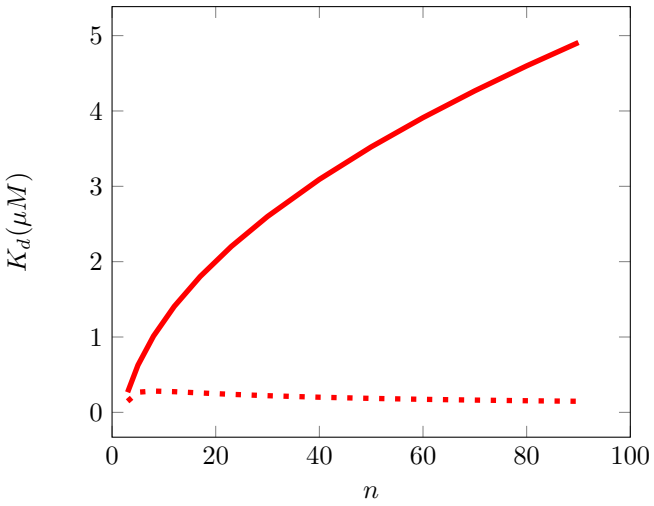

Figure 2.8: The dissociation constant K_d determined from (2.33) (solid line) and (2.34) (dashed line), depending on the p62 oligomer size n. Ubiquitin and p62 oligomer concentrations from Figure 2.6 at the onset of aggregation: $[Ubi] = 1.6\mu M$, $[\text{p62}_n] = 0.4\mu M$.

2.5 Conclusion

In this chapter, we have proposed an ODE model for the growth and decay of aggregates of p62 oligomers cross-linked by ubiquitin chains. Under the assumption of unlimited supply of free oligomers and cross-linkers we found three possible asymptotic regimes: complete degradation of aggregates, convergence towards a finite aggregate size, and unlimited growth (quadratic in time) of the aggregate size. In the latter case, growing aggregates are asymptotically tightly packed with the maximum number of cross-links. These statements are supported by a mixture of explicit steady state computations, formal asymptotic analysis, and numerical simulations. The three regimes, which can be separated explicitly in terms of the reaction constants, have been illustrated by the simulation results. Rigorous proofs of the long-time behaviour in the three regimes are the subject of ongoing investigations.

A comparison of the theoretical results with data from [62] has provided an estimate for the dissociation constant of the elementary reaction between ubiquitin and the UBA domain of p62 in the context of growing aggregates.

There are several possible extensions of this work. A limitation of the original discrete model is that the description of aggregates by triplets (i, j, k) is very incomplete. Typically, very different configurations are described by the same triplet. For example, we could imagine very homogeneous or very heterogeneous aggregates, *i.e.* fully packed in certain regions and very loose in others. Reaction rates will strongly depend on the configuration, including information about the geometry of the aggregate. In principle one can imagine an attempt to overcome these difficulties based on a random graph model [27], but the resulting model describing probability distributions on the sets of all possible aggregate shapes would be prohibitively complex. An intermediate solution would be a more serious approach to finding formulas for quantities like the probability α of losing an oligomer, when a cross-link breaks, based on typical probability distributions.

The model (3.1) describes an intermediate stage of the aggregation process. On the one hand, the large aggregate assumption means that we are dealing with the growth of

already developed aggregates, neglecting the nucleation process, which is important for the number of established aggregates. A model of the nucleation process would be based on the discrete representation and it would have to be stochastic. On the other hand, we neglect two effects important for a later stage of the process. The first and obvious one is the limited availability of free p62 oligomers and ubiquitin cross-linkers. It would be rather straightforward to incorporate this into the model, however at the expense of increased complexity. It would also eliminate the dichotomy between the Cases 1 and 3 of Conjecture 1 since unbounded growth would be impossible. For relatively large initial concentrations of free particles, one could imagine a two-time-scale behaviour with an initial quadratic growth and saturation on a longer time scale. The other effect, which is neglected here but definitely present in experiments, is coagulation of aggregates. This is the subject of ongoing work, based on the PDE model (A.3) derived in the appendix and enriched by an account of the coagulation process.

Chapter 3

Study of a mathematical model of p_{62}-ubiquitin aggregates in autophagy

Contents

This chapter comes from an article that will be submitted soon to Journal of Theoretical Biology *and has been written in collaboration with C. Schmeiser and P. Szmolyan.*

3.1 Introduction

We recall the ODE problem governing the evolution of the state variables:

$$\begin{aligned} \dot p &= (\kappa_1 - \kappa_3 p)(nr - p - 2q) + \kappa_- q\left(1 - \frac{(n-1)p}{(n-2)r}\right) - (\kappa_2 + \kappa_{-1})p\,, && p(0) = p_0\,, \\ \dot q &= \kappa_2 p + \kappa_3 p(nr - p - 2q) - \kappa_- q\,, && q(0) = q_0\,, \\ \dot r &= \kappa_2 p - \kappa_- q\alpha(q,r), \qquad \alpha(q,r) = \frac{nr - 2q}{(n-2)r}\,, && r(0) = r_0\,, \end{aligned} \tag{3.1}$$

with the inequalities

$$nr - p - 2q \geq 0\,, \qquad q \geq r\,, \tag{3.2}$$

implying

$$0 \leq \alpha(q,r) \leq 1\,.$$

We recall from [14, Theorem 1] that for initial data $p_0, q_0, r_0 > 0$ satisfying (3.2), which we assume in the following, the initial value problem (3.1) has a unique, global solution propagating (3.2), the nonnegativity of the components, and in particular

$$r(t), q(t) > 0\,, \qquad t \geq 0\,. \tag{3.3}$$

The search for steady states [14] has suggested a splitting of the parameter space into three regions. Besides the trivial steady state $(p, q, r) = (0, 0, 0)$, only one other equilibrium

may exist, which can be computed explicitly:

$$\bar{p} = \tfrac{\kappa_- A}{\kappa_2}\tfrac{1-\bar{\alpha}}{\bar{\alpha}}\,, \qquad \bar{q} = A\tfrac{1-\bar{\alpha}}{\bar{\alpha}^2}\,, \qquad \bar{r} = \tfrac{2A}{n-(n-2)\bar{\alpha}}\tfrac{1-\bar{\alpha}}{\bar{\alpha}^2}\,, \tag{3.4}$$

$$\text{with} \quad \bar{\alpha} = \tfrac{n}{n-2} + \tfrac{\kappa_{-1}+\kappa_1-\sqrt{(\kappa_1+\kappa_{-1})^2+4\kappa_1\kappa_2(n-1)}}{\kappa_-(n-1)}\,, \quad A = \tfrac{2\kappa_1\kappa_2^2(n-2)}{\kappa_3\kappa_-(\kappa_-(n-1)(n-(n-2)\bar{\alpha})+2\kappa_{-1}(n-2))}\,.$$

Since $\bar{\alpha} = \alpha(\bar{q},\bar{r})$ is the equilibrium value of α, the nontrivial steady state is relevant only in the parameter region defined by $0 < \bar{\alpha} < 1$. It has been conjectured in [14] that in this parameter region $(\bar{p},\bar{q},\bar{r})$ is globally attracting, which has been supported by numerical simulations (see also Chapter 2). Local stability could in principle be examined by linearization. However, the complexity of the resulting formulas has been prohibitive.

Since $(\bar{p},\bar{q},\bar{r}) \to (0,0,0)$ as $\bar{\alpha} \to 1-$, it seems natural to expect a transcritical bifurcation at $\bar{\alpha} = 1$ with stability of the trivial steady state for $\bar{\alpha} > 1$. Again the conjecture of global asymptotic stability of $(0,0,0)$ for $\bar{\alpha} > 1$ has been supported by simulations (see for example Fig. 2.4). The right hand sides of (3.1) are continuous up to the origin (when considered as an element of the set of admissible states), since $0 \le \alpha(q,r) \le 1$ and $p/r \le n$. However, their nonsmoothness prohibits a standard local stability or bifurcation analysis. The expected local stability behaviour (asymptotic stability for $\bar{\alpha} > 1$, instability for $\bar{\alpha} < 1$) is proven in Section 3.2. The analysis is based on a regularizing transformation, which makes the steady state very degenerate, combined with a blow-up analysis [20].

The fact that the components of the nontrivial equilibrium tend to infinity when $\bar{\alpha} \to 0+$ suggests that solutions might be unbounded for $\bar{\alpha} < 0$. In this parameter region approximate solutions with polynomial growth of the form

$$p(t) = p_1 t + o(t)\,, \qquad q(t) = q_2 t^2 + o(t^2)\,, \qquad r(t) = \frac{2q_2}{n}t^2 + o(t^2)\,, \qquad \text{as } t \to \infty\,, \tag{3.5}$$

have been constructed in [14] by formal asymptotic methods. It has also been shown that no other growth behaviour (polynomial with other powers or exponential) should be expected, and the conjecture that all solutions have the constructed asymptotic behaviour is again verified by simulations (see Fig. for example 2.5). We justify the formal asymptotics in Section 3.3. A variant of Poincaré compactification [47] produces a problem with bounded solutions and with three different time scales, which is analyzed by singular perturbation methods [24]. The final result is existence and semi-local stability of the polynomially growing solutions, where 'semi-local' means that initial data have to be large with relative sizes as in (3.5).

The chapter is concluded by a discussion section about biological interpretation of our results as well as perspectives.

3.2 Local stability of the zero steady state

In this section, we study under which conditions small aggregates tend to disaggregate. This is equivalent to studying the stability of the zero-steady-state $(p,q,r) = (0,0,0)$ of the system (3.1). Because of the appearance of the ratios $\frac{p}{r}$ and $\frac{q}{r}$, the Jacobian of the right hand side of (3.1) is not defined there. As a consequence of (3.3) the regularizing transformation $\tau := \int_0^t r(s)^{-1}\mathrm{d}s$ is well defined and leads to

$$\begin{aligned}
\frac{dp}{d\tau} &= r(\kappa_1 - \kappa_3 p)(nr - p - 2q) + \kappa_- q\left(r - \frac{(n-1)p}{n-2}\right) - (\kappa_2 + \kappa_{-1})pr\,,\\
\frac{dq}{d\tau} &= \kappa_2 pr + \kappa_3 pr(nr - p - 2q) - \kappa_- qr\,,\\
\frac{dr}{d\tau} &= \kappa_2 pr - \kappa_- q\frac{nr - 2q}{n-2}\,.
\end{aligned} \tag{3.6}$$

The regularization came at the expense that the zero steady state is degenerate in (3.6), since the right hand side is of second order in terms of the densities. A classical approach

to study such non-hyperbolic points is *blow-up* [20]. The standard blow-up transformation would be the introduction of spherical coordinates, blowing up the origin to the part of $\mathbb{S}^2$ in the positive octant. It is also common to work with *charts* instead. In our case this preserves the polynomial form of the right hand side. It has turned out to be convenient to use the q-chart, whence the blow-up transformation $(p, q, r) \to (p_1, q_1, r_1)$ is given by

$$p = p_1 q_1 \,, \qquad q = q_1 \,, \qquad r = r_1 q_1 \,, \tag{3.7}$$

and we also introduce another change of time scale: $T := \int_0^\tau q_1(\sigma) d\sigma$, again justified by (3.3), leading to

$$\begin{aligned}
\frac{dq_1}{dT} &= q_1 r_1 \left(\kappa_2 p_1 - \kappa_-\right) + \kappa_3 p_1 r_1 q_1^2 (n r_1 - p_1 - 2) \,, \\
\frac{dp_1}{dT} &= r_1(\kappa_1 - \kappa_3 p_1 q_1)(n r_1 - p_1 - 2) + \kappa_- \left(r_1 - \frac{n-1}{n-2} p_1\right) - (\kappa_2 + \kappa_{-1}) p_1 r_1 - p_1 r_1 (\kappa_2 p_1 - \kappa_-) \\
&\quad - \kappa_3 p_1^2 r_1 q_1 (n r_1 - p_1 - 2) \,, \\
\frac{dr_1}{dT} &= (1 - r_1) \left(\kappa_2 p_1 r_1 + \kappa_- \left(\frac{2}{n-2} - r_1\right)\right) - \kappa_3 p_1 r_1^2 q_1 (n r_1 - p_1 - 2) \,.
\end{aligned} \tag{3.8}$$

The invariant manifold $q_1 = 0$ of this system corresponds to the zero steady state of (3.1). The inequalities (3.2) become

$$r_1 \le 1 \,, \qquad 0 \le p_1 \le n r_1 - 2 \,,$$

in terms of the new variables, i.e. the dynamics of (p_1, r_1) remains in the triangle depicted in Fig. 3.1. Since $r_1 \ge 2/n$, we conclude from the equation for q_1 that the invariant manifold is locally exponentially attracting in the region to the left of the line $p_1 = \kappa_-/\kappa_2$. Since $p_1 \le n - 2$, the inequality $\kappa_- > (n-2)\kappa_2$ already implies local asymptotic stability of the invariant manifold $q_1 = 0$ of (3.8) and therefore of the zero steady state of (3.1). Note that $\kappa_- > (n-2)\kappa_2$ also implies $\bar\alpha > 1$ for $\bar\alpha$ defined by (3.4).

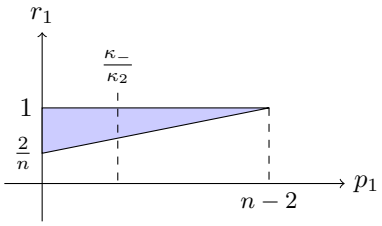

Figure 3.1: The dynamics in the (p_1, r_1)-plane is limited to the shaded triangle because of the inequalities (3.2).

In the following we therefore consider the case $\kappa_- \le (n-2)\kappa_2$ (see Fig. 3.1) and $\bar\alpha > 1$, where the latter is equivalent to

$$\kappa_1 \kappa_2 (n-2)^2 < \kappa_-(\kappa_1 + \kappa_{-1})(n-2) + \kappa_-^2 (n-1) \,, \tag{3.9}$$

see also [14, Equ. (26)]. The flow on the invariant manifold $q_1 = 0$ of (3.8) is governed by the system

$$\begin{aligned}
\frac{dp_1}{dT} &= r_1 \kappa_1 (n r_1 - p_1 - 2) + \kappa_- \left(r_1 - \frac{n-1}{n-2} p_1\right) - (\kappa_2 + \kappa_{-1}) p_1 r_1 - p_1 r_1 (\kappa_2 p_1 - \kappa_-) \\
\frac{dr_1}{dT} &= (1 - r_1) \left(\kappa_2 p_1 r_1 + \kappa_- \left(\frac{2}{n-2} - r_1\right)\right) \,.
\end{aligned} \tag{3.10}$$

In the right part of the triangle, i.e. for

$$r_1 \le 1\,, \qquad \frac{\kappa_-}{\kappa_2} \le p_1 \le nr_1 - 2\,,$$

we have

$$\begin{aligned}\frac{dp_1}{dT} &\le r_1\kappa_1\left(n - \frac{\kappa_-}{\kappa_2} - 2\right) + \kappa_-\left(r_1 - \frac{n-1}{n-2}\,\frac{\kappa_-}{\kappa_2}\right) - (\kappa_2 + \kappa_{-1})\frac{\kappa_-}{\kappa_2}r_1 \\ &= \frac{r_1\big(\kappa_1\kappa_2(n-2)^2 - \kappa_-(\kappa_1+\kappa_{-1})(n-2)\big) - \kappa_-^2(n-1)}{\kappa_2(n-2)} < \frac{(r_1-1)\kappa_-^2(n-1)}{\kappa_2(n-2)} \le 0\,,\end{aligned}$$

where the strict inequality is due to (3.9). This implies that all trajectories reach the left part of the triangle, i.e. $p_1 < \kappa_-/\kappa_2$ in finite time.

By standard regular perturbation theory the dynamics for the full system (3.8), when started close to the invariant manifold $q_1 = 0$, remains close to the dynamics on the invariant manifold for finite time, until the region $p_1 < \kappa_-/\kappa_2$ is reached, where the invariant manifold is attracting. Thus $q = q_1$ tends to zero and, by the inequalities (3.2), the same is true for p and r.

Now we consider the case $\bar\alpha < 1$, i.e. the opposite of inequality (3.9), and look for a steady state on the invariant manifold $r_1 = 1$ of the system (3.10). Since

$$\begin{aligned}\frac{dp_1}{dT}\Big|_{r_1=1,p_1=\kappa_-/\kappa_2} &= \frac{\kappa_1\kappa_2(n-2)^2 - \kappa_-(\kappa_1+\kappa_{-1})(n-2) - \kappa_-^2(n-1)}{\kappa_2(n-2)} > 0\,, \\ \frac{dp_1}{dT}\Big|_{r_1=1,p_1=n-2} &= -(n-2)(n\kappa_2 + \kappa_{-1}) < 0\,,\end{aligned}$$

there exists a steady state $(p_1, r_1) = (p_1^*, 1)$ with $\kappa_-/\kappa_2 < p_1^* < n-2$, which is stable under the flow along $r_1 = 1$. On the other hand

$$\frac{1}{1-r_1}\,\frac{dr_1}{dT}\Big|_{r_1=1,p_1=p_1^*} = \left(\kappa_2 p_1^* + \kappa_-\left(\frac{2}{n-2} - 1\right)\right) > \frac{2\kappa_-}{n-2} > 0\,,$$

which implies stability of the manifold $r_1 = 1$ close to the steady state, and therefore stability of the steady state. The existence of a stable steady state on the invariant manifold $q_1 = 0$ of (3.8) in the region, where the manifold is repulsive, implies instability of the manifold and therefore also of the zero steady state of (3.1). This completes the proof of the main result of this section.

Theorem 5. *Let $\bar\alpha$ be defined by (3.4). Then the steady state $(0,0,0)$ of the system (3.1) is locally asymptotically stable for $\bar\alpha > 1$ and unstable for $\bar\alpha < 1$.*

3.3 Polynomially growing regime

The goal of this section is a rigorous justification of the formal asymptotics (3.5) (see [14]) under the assumption $\bar\alpha < 0$ with $\bar\alpha$ defined in (3.4), i.e.

$$4\kappa_1\kappa_2(n-2)^2 > n\kappa_-\big(2(\kappa_1+\kappa_{-1})(n-2) + \kappa_- n(n-1)\big)\,, \tag{3.11}$$

see also [14, Equ. (27)].

Considering (3.5), it would be natural to write an equation for $p(t)/t$. It is easily seen from (3.1) that its derivative contains terms of the order of t^2. Similarly the derivative of $q(t)/t^2$ has contributions up to the order of t, whereas the derivative of $r(t)/t^2$ is a combination of terms bounded as $t \to \infty$. This shows that we are confronted with a problem with different time scales, which will put us into the realm of *singular perturbation theory* (see, e.g. [24, 56]). The leading order term in the fastest equation, i.e. the p-equation, is

$-\kappa_3 p(nr-2q)$, from which it has been concluded in [14] that $nr(t) \approx 2q(t)$ as $t \to \infty$. In a standard singular perturbation setting, it should be possible to express $p(t)$ from this relation. Since this is not the case, our problem belongs to the family of *singular* singularly perturbed problems (see e.g. [52]) which, however, can be transformed to the standard regular form in many cases.

The introduction of $p(t)/t$, $q(t)/t^2$, $r(t)/t^2$, as new variables would lead to a study of bounded solutions, but to a non-autonomous system. We shall use a variant of the *Poincaré compactification* method [47] instead.

The previous observations led us to the introduction of the new variables

$$u = \frac{p}{\sqrt{p+q}}\,, \qquad v = \frac{2p+2q-nr}{\sqrt{p+q}}\,, \qquad w = \frac{1}{\sqrt{p+q}}\,,$$

where we expect that $w(t)$ tends to zero as t^{-1}, and that $u(t)$ and $v(t)$ converge to nontrivial limits. Since this coordinate change produces a singularity at $w=0$, we also change the time variable by $\tau = \int_0^t ds/w(s)$. In terms of the new variables system (3.1) becomes

$$\begin{aligned}
\frac{du}{d\tau} &= (\kappa_1 w - \kappa_3 u)(u-v) + \kappa_-(1-uw)\left(1 - \frac{n(n-1)uw}{(n-2)(2-vw)}\right) - (\kappa_2+\kappa_{-1})uw \\
&\quad -uw^2 A(u,v,w)\,, \\
\frac{dv}{d\tau} &= w\left(2\kappa_1(u-v) - (2\kappa_{-1}+n\kappa_2)u + \kappa_-(1-uw)n\frac{2u-nv}{(n-2)(2-vw)}\right) - vw^2 A(u,v,w)\,, \\
\frac{dw}{d\tau} &= -w^3 A(u,v,w)\,, \quad A(u,v,w) := \frac{1}{2}\left(\kappa_1(u-v) - \kappa_{-1}u - \kappa_-(1-uw)\frac{n(n-1)u}{(n-2)(2-vw)}\right).
\end{aligned} \tag{3.12}$$

Our goal is to prove that solutions converge to a steady state (u^*, v^*, w^*) with $w^* = 0$, which obviously has to satisfy $-\kappa_3 u^*(u^*-v^*) + \kappa_- = 0$, implying

$$u^* = U(v^*) := \frac{1}{2}\left(v^* + \sqrt{(v^*)^2 + 4\kappa_-/\kappa_3}\right)\,, \tag{3.13}$$

since we need $u^* > 0$. We intend to show that v^* is determined from the requirement that the large parenthesis in the v-equation vanishes. The argument is essentially that for small values of w, the variable v evolves much faster than w.

In order to make the slow-fast structure of this system more apparent and to allow the application of basic results from singular perturbation theory, we assume that the initial value for w is small and define $\varepsilon := (p_0+q_0)^{-1/2} \ll 1$ and the rescaled variable $W = w/\varepsilon$, leading to

$$\begin{aligned}
\frac{du}{d\tau} &= -\kappa_3 u(u-v) + \kappa_- + O(\varepsilon)\,, \\
\frac{dv}{d\tau} &= \varepsilon W\left(2\kappa_1(u-v) - (2\kappa_{-1}+n\kappa_2)u + \kappa_- n\frac{2u-nv}{2(n-2)}\right) + O(\varepsilon^2)\,, \\
\frac{dW}{d\tau} &= -\varepsilon^2 W^3 A(u,v,0) + O(\varepsilon^3)\,.
\end{aligned} \tag{3.14}$$

The initial data are denoted by

$$u(0) = u_0 := \frac{p_0}{\sqrt{p_0+q_0}} > 0\,, \qquad v(0) = v_0 := \frac{2p_0+2q_0-nr_0}{\sqrt{p_0+q_0}}\,, \qquad W(0) = 1\,,$$

where in the following we consider u_0 and v_0 as fixed when $\varepsilon \to 0$. This is a singular perturbation problem in standard form, where τ plays the role of an initial layer variable. We pass to the limit $\varepsilon \to 0$ to obtain the initial layer problem

$$\begin{aligned}
\frac{d\hat{u}}{d\tau} &= -\kappa_3 \hat{u}(\hat{u}-\hat{v}) + \kappa_-\,, \\
\frac{d\hat{v}}{d\tau} &= \frac{d\hat{W}}{d\tau} = 0\,,
\end{aligned} \tag{3.15}$$

subject to the initial conditions. By the qualitative behaviour of the right hand side of the first equation, the solution satisfies $\hat{v}(\tau) = v_0$, $\hat{W}(\tau) = 1$, and

$$\lim_{\tau\to\infty} \hat{u}(\tau) = U(v_0)\,,$$

with exponential convergence, where U has been defined in (3.13). The equation $u = U(v)$ defines the so called *reduced manifold*. Since it is exponentially attracting, the Tikhonov theorem [58] (or rather its extension [24]) implies that, after the initial layer, i.e. when written in terms of the slow variable $\sigma = \varepsilon\tau$, the solution trajectory remains exponentially close to the *slow manifold*, which is approximated by the reduced manifold, and the flow on the slow manifold satisfies

$$\begin{aligned} \frac{dv}{d\sigma} &= W\left(2\kappa_1(U(v)-v) - (2\kappa_{-1}+n\kappa_2)U(v) + \kappa_- n\frac{2U(v)-nv}{2(n-2)}\right) + O(\varepsilon)\,,\\ \frac{dW}{d\sigma} &= -\varepsilon W^3 A(U(v),v,0) + O(\varepsilon^2)\,, \end{aligned} \tag{3.16}$$

with $v(0) = v_0$, $W(0) = 1$. This is again a singular perturbation problem in standard form, where now σ is the initial layer variable. We repeat the above procedure and consider the limiting layer problem

$$\begin{aligned} \frac{d\tilde{v}}{d\sigma} &= \tilde{W}\left(2\kappa_1(U(y\tilde{v})-\tilde{v}) - (2\kappa_{-1}+n\kappa_2)U(\tilde{v}) + \kappa_- n\frac{2U(\tilde{v})-n\tilde{v}}{2(n-2)}\right)\,,\\ \frac{d\tilde{W}}{d\sigma} &= 0\,. \end{aligned} \tag{3.17}$$

The observations

$$U(-\infty) = 0\,, \qquad U(\infty) = \infty\,, \qquad 0 < U'(v) < 1\,,$$

suffice to show that the right hand side of the first equation is a strictly decreasing function of v with a unique zero v^*, which can actually be computed explicitly:

$$v^* = B\left(\kappa_1 - \kappa_{-1} - \frac{n}{2}\kappa_2 + \frac{n}{2(n-2)}\kappa_-\right)$$

with $\quad B = 2\sqrt{\dfrac{\kappa_-}{\kappa_3}}\left(\dfrac{n^3}{4(n-2)}\kappa_-^2 + 4\kappa_1\kappa_{-1} + 2n\kappa_1\kappa_2 + n\kappa_1\kappa_- + \dfrac{n^2}{n-2}\kappa_{-1}\kappa_- + \dfrac{n^3}{2(n-2)\kappa_2\kappa_-}\right)^{-1/2}$

The solution of (3.17) with $\tilde{v}(0) = v_0$ satisfies $\lim_{\sigma\to\infty}\tilde{v}(\sigma) = v^*$ with exponential convergence. Another application of the Tikhonov theorem shows that the slowest part of the dynamics with $t = O(\varepsilon^{-1})$ can be approximated by

$$\frac{dW}{d\sigma} = -\varepsilon W^3 A^*\,, \qquad W(0) = 1\,, \tag{3.18}$$

with

$$A^* := A(U(v^*),v^*,0) = \frac{nB}{16(n-2)^2}(4(n-2)^2\kappa_1\kappa_2 - 2n(n-2)\kappa_-(\kappa_1+\kappa_{-1}) - n^2(n-1)\kappa_-^2) > 0\,, \tag{3.19}$$

by (3.11). This gives the approximation

$$W(\sigma) = (1 + 2A^*\varepsilon\sigma)^{-1/2}\,.$$

The results of [24] imply that the approximations are accurate with errors of order ε uniformly with respect to time.

Theorem 6. *Let (3.11) hold. Then, for $\varepsilon > 0$ small enough, the solution of (3.12) with initial conditions*

$$u(0) = u_0 > 0\,, \qquad v(0) = v_0 \in \mathbb{R}\,, \qquad w(0) = \varepsilon\,,$$

satisfies

$$\begin{aligned} u(\tau) &= \hat{u}(\tau) - U(v_0) + U(\tilde{v}(\varepsilon\tau)) + O(\varepsilon)\,, \\ v(\tau) &= \tilde{v}(\varepsilon\tau) + O(\varepsilon)\,, \\ w(\tau) &= \varepsilon(1 + 2A^*\varepsilon^2\tau)^{-1/2} + O(\varepsilon^2)\,, \end{aligned}$$

uniformly in $\tau \geq 0$, where U is given in (3.13), $\hat{u}$ solves (3.15), $\tilde{v}$ solves (3.17), and A^* is given in (3.19).

Actually more can be deduced. In terms of the original time variable t, the equation for w in (3.12) becomes

$$\dot{w} = -w^2 A(u, v, w)\,. \tag{3.20}$$

Under the assumptions of Theorem 6, $A(u, v, w)$ is uniformly close to the positive constant A^* and therefore uniformly positive for large enough t. This implies that w tends to zero as $t \to \infty$. The slow manifold of the system (3.16) reduces to the steady state $(v, W) = (v^*, 0)$ for $W = 0$. Therefore v tends to v^* as $t \to \infty$. Analogously, the slow manifold of (3.14) reduces to the steady state $(u, v, W) = (u^* = U(v^*), v^*, 0)$ at $W = 0$, implying convergence of u to u^*. This in turn implies convergence of $A(u, v, w)$ to A^*, which can be used in (3.20).

Corollary 1. *Let the assumptions of Theorem 6 hold. Then*

$$\lim_{t\to\infty} u(t) = u^*\,, \qquad \lim_{t\to\infty} v(t) = v^*\,, \qquad w(t) = \frac{1}{A^* t} + O\left(\frac{1}{t^2}\right) \quad \text{as } t \to \infty\,.$$

Finally, we reformulate these results in terms of the original variables, verifying the formal asymptotics of [14] for initial data, which are in a sense already 'close enough' to the polynomially growing solutions.

Theorem 7. *Let (3.11) hold, let $c_2 \geq c_1 > 0$, and let $\delta > 0$ be small enough. Let the initial data satisfy*

$$p_0 = \frac{c_1}{\delta}\,, \qquad q_0 = \frac{1}{\delta^2}\,, \qquad r_0 = \frac{2}{n\delta^2} + \frac{c_2}{n\delta}$$

Then the solution of (3.1) with $(p(0), q(0), r(0)) = (p_0, q_0, r_0)$ satisfies

$$p(t) = u^* A^* t + o(t)\,, \qquad q(t) = (A^*)^2 t^2 + o(t^2)\,, \qquad r(t) = \frac{2}{n}(A^*)^2 t^2 + o(t^2)\,, \qquad \text{as } t \to \infty\,.$$

Proof. We just need to verify that the assumptions of this theorem imply the assumptions of Theorem 6. The result is then a direct consequence of Corollary 1. Actually the assumptions of Theorem 6 hold with $\varepsilon \approx \delta$, since

$$u_0 = \frac{c_1}{\sqrt{1 + c_1\delta}}\,, \qquad v_0 = \frac{2c_1 - c_2}{\sqrt{1 + c_1\delta}}\,, \qquad w_0 = \frac{\delta}{\sqrt{1 + c_1\delta}}\,.$$

□

3.4 Discussion

In this work a mathematical model for aggregation via cross-linking has been analyzed. Besides the basic assumption that aggregating *particles* (here p62 oligomers) need to have at least $n = 3$ binding sites for *cross-linkers* (here ubiqutinated cargo), the rate constants

for binding reactions need to be large enough compared to those for the unbinding reactions (the opposite of inequality (3.9)) for stable aggregates to exist. Under a stronger condition (inequality (3.11)) aggregates grow indefinitely in the presence of an unlimited supply of free particles and cross-linkers. These conjectures from [14], where the model has been formulated, have been partially proven in this work. It has been shown in Section 3.2 that small aggregates get completely degraded under the condition (3.9) and that they grow under the opposite condition. In the latter case, but when (3.11) does not hold, there exists an equilibrium configuration with positive aggregate size. Finally, it has been shown in Section 3.3 that under the condition (3.11) aggregate size grows polynomially with time (actually like t^2) for appropriate initial states.

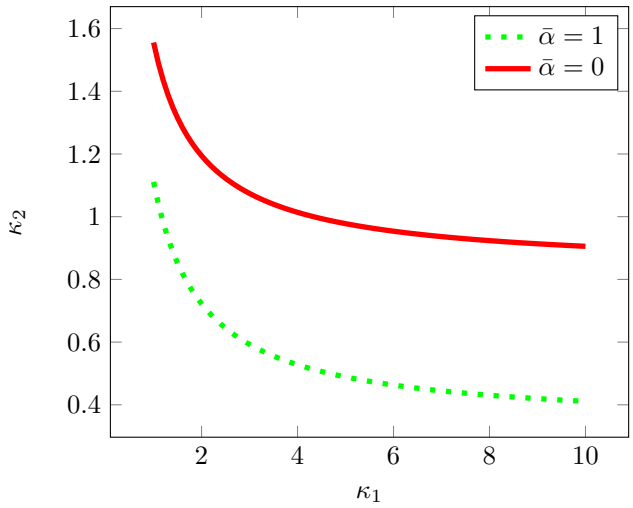

Figure 3.2: Bifurcation diagram obtained for $\kappa_{-1} = \kappa_- = 1$

The constants κ_1, κ_2 in the model have to be interpreted as the products of rate constants with the concentrations of free cross-linkers and, respectively, of free particles. This means that the conditions (3.9) and (3.11) are actually conditions for these concentrations. Fig. 3.2 shows a bifurcation diagram in terms of κ_1 and κ_2 with the curves $\bar{\alpha} = 1$, corresponding to equality in (3.9), and $\bar{\alpha} = 0$, corresponding to equality in (3.11). The qualitative behaviour is no surprise: Close to the origin, i.e. for small concentrations of free particles and cross-linkers, aggregates are unstable. Moving to the right and/or up we pass through two bifurcations to stable finite aggregate size and, subsequently, to polynomial growth of aggregates. Less obvious is the fact that the picture is rather unsymmetric with respect to the two parameters. The condition $(n-2)\kappa_2 > \kappa_-$ is necessary for the existence of stable aggregates, regardless of the value of κ_1, whereas arbitrarily small values of κ_1 can be compensated by large enough κ_2. This means that, if the concentration of free particles is below a threshold, even a large concentration of cross-linkers does not lead to aggregation, whereas arbitrarily small numbers of cross-linkers are used for aggregation if the particle concentration is high. For the application in cellular autophagy this means that aggregation will only happen for large enough concentrations of p62 oligomers. However, arbitrarily small amounts of ubiquitinated cargo can be aggregated in the presence of a large enough supply of oligomers.

This work has been motivated by the experimental results of [63], where aggregates have been detected by light microscopy. If the evolution of single aggregates can be followed, the growth like t^2 might be observed as a fluorescence signal of tagged oligomers, which goes like t^2, or cross section areas going like $t^{4/3}$, if a roughly spherical shape of aggregates is assumed. For quantitative predictions of such experiments, the model should be extended in various ways. First, the *limited supply of free p62 oligomers and of free cross-linkers* should be taken

into account. This is straightforward for the modeling of a single aggregate, but if many aggregates develop simultaneously, they will compete for the free particles. Apart from that the number of aggregates has to be predicted, which requires modeling of the *nucleation* process. Finally, it is very likely that the *coagulation* of aggregates plays an important role. A growth-coagulation model for distributions of aggregates, based on the growth model (3.1) would be prohibitively complex. It is therefore the subject of ongoing work to formulate, analyze, and simulate a growth-coagulation model based on the multiscale analysis of Section 3.3, where aggregates are only described by the size parameter r (number of p62 oligomers in the aggregate), whose evolution is determined by the slow dynamics (3.18), which translates to an equation of the form $\dot{r} = C\sqrt{r}$ for r. This approach raises several challenging issues such as the development of an efficient simulation algorithm or the existence and stability of equilibrium aggregate distributions.

Chapter 4

Improvement of the model and study of transport-coagulation equations

Contents

This chapter is an on-going collaboration with M. Doumic and C. Schmeiser.

4.1 Improved model

We take back the model introduced in Chapter 2 and take into account two new phenomena. Firstly, we consider now that the concentrations of p62 and Ubiquitin (denoted respectively by a and b) evolve with time, which is expressed by including the equations for the conservation of mass (4.2) and (4.3), in contrast with the chapter 2, where these quantities were considered constant over time. Secondly, based on biological observation from G. Zaffagnini, (See *e.g.* in Figure 4.1 from [65]), we decide to consider that aggregates can interact together by coagulating with each other. However, we do not to take into account fragmentation, as according to [65], p62-Ubiquitin aggregates do not behave as liquid droplets, which means that no rearrangement of aggregates are observed, what would be the consequence of fragmentation. This leads to the following nonlocal nonlinear transport-coagulation equation :

$$\partial_t f + \partial_p(V_p f) + \partial_q(V_q f) + \partial_r(V_r f) = Q(f, f) \tag{4.1}$$

with :

$$
\begin{aligned}
V_p &= (\kappa_1 - \kappa_3 p)(nr - p - 2q) + \kappa_- q\left(1 - \frac{(n-1)p}{(n-2)r}\right) - (\kappa_2 + \kappa_{-1})p\,, && p(0) = p_0\,,\\
V_q &= \kappa_2 p + \kappa_3 p(nr - p - 2q) - \kappa_- q\,, && q(0) = q_0\,,\\
V_r &= \kappa_2 p - \kappa_- q\alpha(q,r)\,, && r(0) = r_0\,,
\end{aligned}
$$

where now, $\kappa_1 = \bar{\kappa}_1 a$ and $\kappa_2 = \bar{\kappa}_2 b$, with :

$$a = a_0 - \varepsilon \int_0^\infty (p' + q') f(p', q', r') dp' dq' dr', \tag{4.2}$$

$$b = b_0 - \varepsilon \int_0^\infty r' f(p', q', r') dp' dq' dr', \tag{4.3}$$

$$\tag{4.4}$$

and

$$
\begin{aligned}
&C(f,f) = C_1(f,f) - C_2(f,f),\\
&C_1(f,f) = \frac{1}{2}\int_0^p \int_0^q \int_0^r k(p-p', q-q', r-r', p', q', r') f(t, p-p', q-q', r-r') f(t, p', q', r') dp' dq' dr',\\
&C_2(f,f) = f(t,p,q,r) \int_0^\infty \int_0^\infty \int_0^\infty k(p,q,r,p',q',r') f(t,p',q',r') dp' dq' dr'.
\end{aligned}
$$

The equations (4.2) and (4.3) are derived from the conservation of the mass, $p+q$ (respectively r) corresponding to the amount of Ubiquitin (respectively p62) in the aggregates. The factor ε expresses the fact that in the beginning of the reaction, p62 and Ubiquitin are in large amount, and so can be considered almost as constant. $C(f,f)$ is the coagulation term that has been introduced in the Chapter 1 and k is the associated coagulation kernel. (p,q,r) have to satisfy the inequalities (1.2), which is taken into account in the support of the kernel k. The choice of k can be done following the physical and chemical literature (A review of different models can be found *e.g.* in [50]).

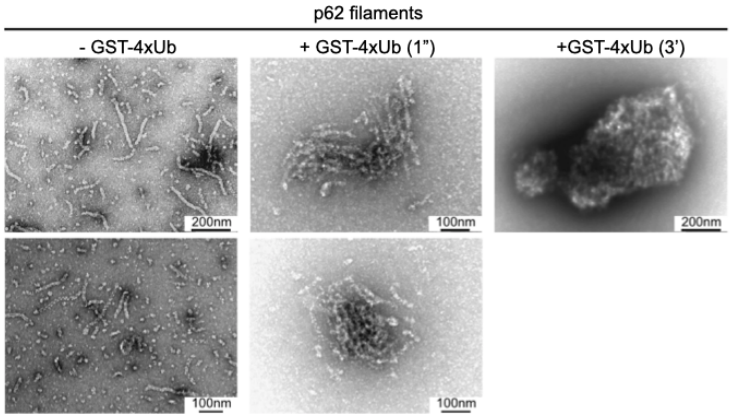

Figure 4.1: Representative electron micrographs of negatively stained p62 filaments incubated in the presence or absence of GST-4xUb for the indicated times. Figure and caption from [65].

4.2 Formal derivation of a one-dimensional transport-coagulation equation from the improved model

In all this section, we use the shorthand notation $\int$ for denoting $\int_0^\infty$.

In this section, we start from (4.1) and derive a one-dimensionaltransport-coagulation equation, using geometric singular perturbation analysis as in Chapter 3. We make the change of variable $(p, q, r) \to (p, x = p + q, y = 2p + 2q - nr)$, which can be related to the variables (u, v, w) used in the Chapter 3 in the following way :

$$u = \frac{p}{x}, \quad v = \frac{y}{x}, \quad \text{and} \quad w = \frac{1}{x},$$

hence (u, v, w) corresponds to the local coordinates of the Poincaré change of variable associated with the variables (p, x, y) in the chart $\mathcal{K}_x$. The new density function $\tilde{f}$ associated with the new variables (p, x, y) is given by $f(p, q, r) = \tilde{f}(p, x, y)$. Consequently, the points along the characteristics of (4.1) satisfy the following nonlocal nonlinear ODE system :

$$\begin{aligned}
V_p =&(\bar{\kappa}_1(\bar{a}_0 - \varepsilon \int x' \tilde{f} dp' dx' dy') - \kappa_3 p)(p - y) + \kappa_-(x - p) \\
&- (\bar{\kappa}_2(\bar{b}_0 - \varepsilon \int \frac{(2x' - y')}{n} \tilde{f} dp' dx' dy') + \kappa_{-1})p \\
V_x =&\bar{\kappa}_1(\bar{a}_0 - \varepsilon \int x' \tilde{f} dp' dx' dy')(p - y) - \kappa_{-1} p - n\kappa_- \frac{(n-1)(x-p)p}{(n-2)(2x-y)} \\
V_y =&2\bar{\kappa}_1(\bar{a}_0 - \varepsilon \int x' \tilde{f} dp' dx' dy')(p - y) - 2\kappa_{-1} p \\
&- n\kappa_2(\bar{b}_0 - \varepsilon \int \frac{(2x' - y')}{n} \tilde{f} dp' dx' dy')p + n\kappa_- \frac{(2p - ny)(x - p)}{(n-2)(2x-y)}.
\end{aligned}$$

The coagulation term reads :

$$\begin{aligned}
&C(\tilde{f}, \tilde{f}) = C_1(\tilde{f}, \tilde{f}) - C_2(\tilde{f}, \tilde{f}), \\
&C_1(\tilde{f}, \tilde{f}) = \frac{1}{2} \int_0^p \int_0^x \int_0^y \tilde{k}(p - p', x - x', y - y', p', x', y') \tilde{f}(t, p - p', x - x', y - y') \tilde{f}(t, p', x', y') dp' dx' dy', \\
&C_2(\tilde{f}, \tilde{f}) = \tilde{f}(t, p, x, y) \int_0^\infty \int_0^\infty \int_0^\infty k(p, x, y, p', x', y') f(t, p', x', y') dp' dx' dy',
\end{aligned}$$

with :

$$\tilde{k}(p, x, y, p', x', y') = \frac{1}{n} k(p, q, r, p', q', r').$$

To make appear different timescales, we make the following change of variable $(p, x, y) \to (P = \sqrt{\varepsilon} p, X = \varepsilon x, Y = \sqrt{\varepsilon} y)$. This allows us to place ourselves artificially close to infinity, as $p, x, y \to \infty$, when $\varepsilon \to 0$. The factor $\sqrt{\varepsilon}$ in front of p and y expresses the assumption to be in the polynomially growing regime, close to infinity, where p and $y = p - (nr - p - 2q)$ grow like t while x grows as q like t^2 *i.e.* like the square of p, hence the factor ε in front of x. The density function reads :

$$F(P, X, Y) = \frac{1}{\varepsilon^2} \tilde{f}(\frac{P}{\sqrt{\varepsilon}}, \frac{X}{\varepsilon}, \frac{Y}{\sqrt{\varepsilon}}).$$

We rescale the coagulation kernel in the following way for convenience :

$$K(P, X, Y, P', X', Y') = \varepsilon \sqrt{\varepsilon} k(p, x, y, p', x', y')$$

and the term of coagulation reads

$$q(F,F) = \sqrt{\varepsilon}\Big(q_1(F,F) - q_2(F,F)\Big),$$

$$q_1(F,F) = \frac{1}{2}\int_0^P \int_0^X \int_0^Y K(P-P', X-X', Y-Y', P', X', Y')F(t,P,X,Y)F(t,P',X',Y')dP'dX'dY',$$

$$q_2(F,F) = F(t,P,X,Y)\int_0^\infty \int_0^\infty \int_0^\infty K(P,X,Y,P',X',Y')F(t,P',X',Y')dP'dX'dY'.$$

Finally, the system of equations transforms into the following equation :

$$\begin{aligned} V_P = \sqrt{\varepsilon}p =& (\bar{\kappa}_1(\bar{a}_0 - \int X'FdP'dX'dY') - \kappa_3\frac{P}{\sqrt{\varepsilon}})(P-Y) + \kappa_-(\frac{X}{\sqrt{\varepsilon}} - P) \\ & - (\bar{\kappa}_2(\bar{b}_0 - \int (2X' - \sqrt{\varepsilon}Y)FdP'dX'dY') + \kappa_{-1})P \\ V_X = \varepsilon x =& \sqrt{\varepsilon}\Big(\bar{\kappa}_1(\bar{a}_0 - \int X'FdP'dX'dY')(P-Y) - \kappa_{-1}P - n\kappa_-\frac{(n-1)(X-\sqrt{\varepsilon}P)P}{(n-2)(2X-\sqrt{\varepsilon}Y)}\Big) \\ V_Y = \sqrt{\varepsilon}y =& 2\bar{\kappa}_1(\bar{a}_0 - \int X'FdP'dX'dY')(P-Y) - 2\kappa_{-1}P - \bar{\kappa}_2(n\bar{b}_0 - \int (2X' - \sqrt{\varepsilon}Y')FdP'dX'dY')P \\ & + n\kappa_-\frac{(2P-nY)(X+\sqrt{\varepsilon}P))}{(n-2)(2X+\sqrt{\varepsilon}Y)}. \end{aligned}$$

We do a first time change of variable $\tau = \frac{t}{\sqrt{\varepsilon}}$, that leads to the following PDE :

$$\partial_\tau F + \sqrt{\varepsilon}\partial_P(V_P F) + \sqrt{\varepsilon}\partial_X(V_X F) + \sqrt{\varepsilon}\partial_Y(V_Y F) = \sqrt{\varepsilon}q(F,F).$$

We let $\varepsilon \to 0$ and obtain that formally on the critical manifold, the following PDE is satisfied :

$$\partial_\tau F + \partial_P\Big((-\kappa_3 P(P-Y) + \kappa_- X)F\Big) = 0. \tag{4.5}$$

The points (P,X,Y) that belong to the characteristics of (4.5) satisfy :

$$\begin{aligned} \tilde{V}_P &= -\kappa_3 P(P-Y) + \kappa_- X, \\ \tilde{V}_X &= 0, \\ \tilde{V}_Y &= 0. \end{aligned}$$

The steady-states (P,X,Y) of the characteristics satisfy :

$$P(X,Y) = \frac{Y}{2} + \sqrt{\frac{Y^2}{4} + \frac{\kappa_- X}{\kappa_3}}. \tag{4.6}$$

We can now integrate over P, using the formula (4.6) and the assumption that $\lim_{P\to\infty} F(\tau,P,X,Y) = 0$, which leads to :

$$\begin{aligned} &\int \partial_\tau F dP + \sqrt{\varepsilon}\int \partial_X(V_X F)dP + \sqrt{\varepsilon}\int \partial_Y(V_Y F)dP \\ &= \sqrt{\varepsilon}\int q(F,F)dP. \end{aligned}$$

Let us introduce $g = \int F dP$, so that we obtain :

$$\partial_\tau g + \sqrt{\varepsilon}\partial_X(V_X g) + \sqrt{\varepsilon}\partial_Y(V_Y g) = \sqrt{\varepsilon}Q(g,g),$$

with $Q(g,g) = \int q(F,F)dP$. We make the time change of variable $\tau \to t$. Let $\varepsilon \to 0$, then we obtain formally that on the critical manifold, the following PDE is satisfied :

$$\partial_t g + \partial_Y(\hat{V}_Y h) = 0.$$

The characteristics of this PDE satisfy the following ODE :

$$\hat{V}_Y = 2\bar{\kappa}_1(\bar{a}_0 - \int XFdPdXdY)(P-Y) - 2\kappa_{-1}P - \bar{\kappa}_2 n\bar{(}b_0 - 2\int XFdPdXdY)P + \frac{n\kappa_-}{2(n-2)}(2P - nY),$$

$$\hat{V}_X = 0.$$

After a straightforward computation using the fact that P is given by (4.6), we obtain the following formula for the steady-states of the previous characteristics :

$$Y = v^*\sqrt{X}. \tag{4.7}$$

with v^* has been defined previously in Chapter 3. We draw the attention of the reader toward the fact that v^* is not anymore a constant as in the Chapter 3 but a nonlocal term (because of the term $\int XFdPdXdY$). We integrate now over Y. In order to do so, we introduce as previously $G = \int gdY = \int\int FdPdY$, and make a new change of variable $t \to \sigma = \sqrt{\varepsilon}t$, which leads to :

$$\partial_\sigma G + \partial_X(\bar{V}_X G) = \mathcal{Q}(G,G),$$

where

$$\begin{aligned}
\mathcal{Q}(G,G) &= \mathcal{Q}_1(G,G) - \mathcal{Q}_2(G,G),\\
\mathcal{Q}_1(G,G) &= \frac{1}{2}\int_0^X K(X-X',X')G(t,X-X')G(t,X')dX',\\
\mathcal{Q}_2(G,G) &= G(t,X)\int_0^\infty K(X,X')G(t,X')dX'.
\end{aligned}$$

Replacing P and Y, by their expressions (4.6) and (4.7), we can compute straightforwardly :

$$\bar{V}_X = A^*\sqrt{X},$$

with A^* defined in Chapter 3, which is now a nonlocal term similarly as v^*. Finally, we derived formally the following one-dimensional nonlocal transport-coagulation equation :

$$\partial_t G + \partial_X(A^*\sqrt{X}G) = \mathcal{Q}(G,G).$$

with A^* whose sign depends on the value of the nonlocal term $\int X'FdP'dX'dY'$.

4.3 Study of a general one-dimensional transport-coagulation equation

The one-dimensionaltransport-coagulation equation derived in the previous section can be simplified as (4.9) (we don't take into account the non-local term). Our first aim is to explore the necessary and sufficient conditions of the existence of a non-trivial steady state of (4.9). Having a non-trivial steady state implies both the conservation of the number of particles in Equation (4.10) and the conservation of the mass in Equation (4.11). This leads us to impose first $v(0)f_0 > 0$, in order to compensate the loss of particles due to coagulation in (4.10), and second the sign of $v(x)$ must change so that $\int v(x)f(x)dx = 0$ is made possible in Equation (4.11). Furthermore, it is necessary to have a negative speed for large x in order

to compensate the coagulation term that gives rise to increasingly larger particles. As the simplest way to satisfy all these assumptions, we choose a C^1 decreasing function $v(x)$ such that

$$\begin{aligned} v(x) &> 0, \qquad \text{for} \quad x < x_0 \\ v(x_0) &= 0, \qquad \text{for} \quad x_0 > 0 \\ v(x) &< 0, \qquad \text{for} \quad x > x_0 \end{aligned} \tag{4.8}$$

Further assumptions on the decay rate of $v(x)$ at $+\infty$ may be required (see e.g. Section 4.5 for the case of the multiplicative kernel).

4.3.1 Model

Let $f_0 > 0$, $v(x)$ a C^1 decreasing function and $x_0 > 0$ such that $v(x_0) = 0$, $K(x, y)$ a symetric coagulation kernel - we shall consider here only $K(x, y) = 2$, $K(x, y) = x + y$ and $K(x, y) = xy$. We consider the following system:

$$\begin{cases} \frac{\partial}{\partial t} f(x,t) + \frac{\partial}{\partial x}\big(v(x) f(x,t)\big) = & \frac{1}{2} \int_0^x K(x-y,y) f(x-y,t) f(y,t) dy \\ & - \int_0^\infty K(x,y) f(y,t) f(x,t) dy, \\ f(0,t) = f_0. \end{cases} \tag{4.9}$$

4.3.2 Balance equations

Integrating the equation, we find a balance equation for the number of particles

$$\frac{d}{dt} \int_0^\infty f(x,t) dx = v(0) f_0 - \frac{1}{2} \int_0^\infty \int_0^\infty K(x,y) f(x,t) f(y,t) dx dy, \tag{4.10}$$

and integrating the equation against the weight x, we have another balance equation for the mass

$$\frac{d}{dt} \int_0^\infty x f(x,t) dx = \int_0^\infty v(x) f(x,t) dx. \tag{4.11}$$

4.3.3 Examples of steady states

Before looking for necessary and sufficient conditions of the existence of steady states, let us consider some cases where the explicit steady state $f_0 e^{-x}$ is admissible:

1. for $K(x, y) = 2$: if $v(x) = f_0(1 - x)$,
2. for $K(x, y) = x + y$: if $v(x) = f_0(1 - \frac{x^2}{2})$,
3. for $K(x, y) = xy$: if $v(x) = f_0(\frac{1+x}{2} - \frac{x^2}{4} - \frac{x^3}{12})$.

4.4 Results with constant kernel

For the constant kernel $K(x, y) = 2$, we are able to compute all the moments associated with the density function.

4.4.1 Equation for the zero order moment

The equation (4.10) leads us to the following equation for $\mu_0(t) = \int_0^\infty f(x,t) dx$:

$$\frac{d}{dt} \mu_0 = v(0) f_0 - \mu_0^2.$$

Defining $u = e^{\int_0^t \mu_0(s)ds}$, we have

$$u''(t) = v(0)f_0 u(t), \qquad u(0) = 1, \qquad u'(0) = \mu_0(0),$$

hence we have, with $\alpha = \sqrt{v(0)f_0}$,

$$u(t) = \cosh(\alpha t) + \frac{\mu_0(0)}{\alpha}\sinh(\alpha t),$$

so that

$$\mu_0(t) = \frac{\alpha \sinh(\alpha t) + \mu_0(0)\cosh(\alpha t)}{\cosh(\alpha t) + \frac{\mu_0(0)}{\alpha}\sinh(\alpha t)} \to_{t\to\infty} \alpha = \sqrt{v(0)f_0}.$$

4.4.2 Equation for higher-order moments

The equation (4.10) leads to the following equation for $\mu_k(t) = \int_0^\infty x^k f(x,t)dx$ with $k \in \mathbb{N}^*$:

$$\frac{d}{dt}\mu_k(t) + \int_0^\infty x^k \partial_x(vf)dx = \int_0^\infty x^k \int_0^x f(x-y,t)f(y,t)dydx - 2\int_0^\infty x^k f(x,t)dx \int_0^\infty f(y,t)dy,$$

hence

$$\frac{d}{dt}\mu_k(t) - k\int_0^\infty x^{k-1}(b_0 - 2x)f(x)dx = \int_0^\infty \int_0^x (x-y+y)^k f(x-y,t)f(y,t)dydx - 2\mu_k(t)\mu_0(t).$$

This equation can be rewritten using the binomial theorem :

$$\frac{d}{dt}\mu_k(t) - kb_0\mu_{k-1}(t) + 2k\mu_k(t) = \sum_{i=0}^{k}\int_0^\infty \int_0^x \binom{k}{i}(x-y)^i y^{k-i} f(x-y,t)f(y,t)dydx - 2\mu_k(t)\mu_0(t),$$

hence

$$\frac{d}{dt}\mu_k(t) - kb_0\mu_{k-1}(t) + 2k\mu_k(t) = \sum_{i=0}^{k}\binom{k}{i}\mu_i(t)\mu_{k-i}(t) - 2\mu_k(t)\mu_0(t),$$

hence

$$\frac{d}{dt}\mu_k(t) + 2k\mu_k(t) = \sum_{i=1}^{k-1}\binom{k}{i}\mu_i(t)\mu_{k-i}(t) + kb_0\mu_{k-1}(t),$$

which is an ODE for the variable $\mu_k(t)$ in terms of all the moments $(\mu_i(t))_{i=1,\dots,k-1}$, with $\mu_0(t)$ that has been previously determined (See 4.4.1). Thus, all the moments for the constant kernel can be computed by induction. Assuming by induction that all the moments μ_i for $i \le k-1$ remain bounded and converge to a constant at large times, we have

$$\frac{d}{dt}(\mu_k e^{2kt}) = e^{2kt}F(t),$$

with F a nonnegative bounded function, hence

$$\mu_k(t) = e^{-2kt}(\mu_1(0) + \int_0^t F(s)e^{2ks}ds) \le \mu_1(0) + \frac{1}{2k}\max(F),$$

so that μ_k remains positive and bounded. We easily prove that any sequence $\mu_k(t_n)$ with $t_n \to \infty$ is a Cauchy sequence, hence μ_k converges to a positive limit, defined by induction by

$$\bar{\mu}_k = \frac{1}{2k}\sum_{i=1}^{k-1}\binom{k}{i}\bar{\mu}_i\bar{\mu}_{k-i} + \frac{b_0}{2}\bar{\mu}_{k-1}. \tag{4.12}$$

This constitutes a Stieltjes moment problem (See [53]), that we have not solved yet.

4.5 Results for the multiplicative kernel

We now consider the equation (4.9) for the kernel $K(x,y) = xy$. We aim to prove the existence and the uniqueness of a steady-state using a fix point argument provided some assumptions on the transport-speed. In this case, the transport counters the coagulation, similarly as it has been shown in other papers that fragmentation could counter coagulation under specific conditions. In the case of the multiplicative kernel, the transport-coagulation rewrites :

$$\begin{aligned} &\partial_t f + \partial_x(vf) = \frac{1}{2}\int_0^x (x-y)f(x-y)yf(y)dy - \int_0^\infty xf(x)yf(y)dy\,, \\ &f(0,t) = f_0. \end{aligned} \tag{4.13}$$

We work in the following Banach space :

$$\mathcal{B} = \left\{ f : \int_0^\infty xf(x)dx < \infty \right\}.$$

Theorem 8. *Assuming that $v(x) = (x_0 - x)w(x)$ with $w(x) > 0$ smooth, $v(x)$ decreases in $+\infty$ at least as x^{-2} with $2 > 2$, $f_0 \in \mathcal{B}$, then, there exists a unique steady state of (4.13).*

We consider the sequence $\left(f_n\right)_{n\in\mathbb{N}}$ defined by :

$$\partial_x(vf^{n+1}) + xf^{n+1}M_1(f^n) = h_n(x) = \frac{1}{2}\int_0^x (x-y)f^n(x-y)yf^n(y)dy\,, \qquad f^{n+1}(0) = f_0\,. \tag{4.14}$$

Let us assume that there exists an $n \in \mathbb{N}$ s.t. $f_n \in \mathcal{B}$. For $0 \le x < x_0$ we get (by writing the equation for vf^{n+1} and by variation of constants) that :

$$f^{n+1}(x) = \frac{v(0)f_0}{v(x)}G(x) + \frac{1}{v(x)}\int_0^x \frac{G(x)}{G(y)}h_n(y)dy\,,$$

with

$$\begin{aligned} G(x) &= \exp\left(-M_1(f^n)\int_0^x \frac{y}{v(y)}dy\right) \\ M_1(f^n) &= \int_0^\infty xf^n(x)dx. \end{aligned}$$

Using the assumption,

$$v(x) = (x_0 - x)w(x) \tag{4.15}$$

with $w(x) > 0$ smooth, it follows that :

$$\begin{aligned} \int_0^x \frac{y}{v(y)}dy &= \frac{x_0}{w(x_0)}\int_0^x \frac{dy}{x_0 - y} + \int_0^x \frac{1}{x_0 - y}\left(\frac{y}{w(y)} - \frac{x_0}{w(x_0)}\right)dy \\ &= -\frac{x_0}{w(x_0)}\log(x_0 - x) + b(x)\,, \end{aligned}$$

where $b(x)$ is a smooth function (up to $x = x_0$). Hence

$$\frac{G(x)}{v(x)} = (x_0 - x)^{\frac{M_1(f^n)x_0}{w(x_0)} - 1}c(x)\,,$$

where $c(x) > 0$ is again a smooth function. It is always integrable, since the exponent is always larger than -1. Finally, assuming $f^n \in \mathcal{B}$, we have that :

$$\int_0^{x_0} xf^{n+1}(x)dx < \infty$$

For $x > x_0$, we get similarly as before that :

$$f^{n+1}(x) = -\frac{1}{v(x)} \int_x^{+\infty} \frac{G(x)}{G(y)} h_n(y) dy \,,$$

with

$$G(x) = \exp\left(-M_1(f^n) \int_x^{+\infty} \frac{y}{v(y)} dy \right) .$$

The existence of G requires that v decreases at least like $x^{-\gamma}$ in $+\infty$ with $\gamma > 2$. Under this condition, G is then a decreasing function. To prove $f^{n+1} \in \mathcal{B}$, we need to check the integrability of $xf(x)$ in x_0 and in $+\infty$. The integrability in x_0 is guaranteed by the former assumption (4.15). Let us now consider what is happening in $+\infty$. The integral is convergent, if it decreases in the following polynomial manner, namely if $xf^{n+1}(x) \leq \frac{1}{1+x^\gamma}$ with $\gamma > 1$. Hereafter, we show by induction that for x close enough to $+\infty$, for all $n \in \mathbb{N}$, it holds that :

$$f^n(x) \leq \frac{A}{(1+x)^\alpha}, \tag{4.16}$$

for $\alpha > 2$. Assuming (4.16), it follows that,

$$\begin{aligned}
h_n(y) \leq & \frac{A^2}{2} \int_0^y (y-z) z (1+y-z)^{-\alpha} (1+z)^{-\alpha} dz \\
h_n(y) \leq & \frac{A^2 y^3}{3} \int_0^1 (1-w) w (1+y(1-w))^{-\alpha} (1+yw)^{-\alpha} dw \\
h_n(y) \leq & \frac{A^2 y^3}{3} (1+\frac{y}{2})^{-\alpha} (\int_0^{\frac{1}{2}} \frac{w}{(1+yw)^\alpha} dw + \int_{\frac{1}{2}}^1 \frac{1-w}{(1+y(1-w))^\alpha} dw) \\
h_n(y) \leq & \frac{A^2 y^3}{3} (1+\frac{y}{2})^{-\alpha} \frac{1}{y} \int_0^{\frac{1}{2}} ((1+yw)^{1-\alpha} - (1+yw)^{-\alpha}) dw \\
h_n(y) \leq & \frac{A^2 y}{3} (1+\frac{y}{2})^{-\alpha} [(\frac{(1+yw)^{2-\alpha}}{2-\alpha} - \frac{(1+yw)^{1-\alpha})}{1-\alpha}]_0^{\frac{1}{2}} \\
h_n(y) \leq & \frac{A^2 y}{3} (1+\frac{y}{2})^{-\alpha} (\frac{1}{1-\alpha} - \frac{1}{2-\alpha} + O(1)) \\
h_n(y) \leq & A y (1+\frac{y}{2})^{-\alpha} (\frac{1}{(\alpha-1)(\alpha-2)} + O(1)).
\end{aligned}$$

Finally, assuming that $|v(x)| < Bx^{-2}$,

$$\begin{aligned}
f^{n+1}(x) &\leq \frac{1}{Bx^2} \int_x^{+\infty} \frac{A^2 2^\alpha}{(\alpha-1)(\alpha-2)} y^{1-\alpha} dy \\
f^{n+1}(x) &\leq x^{2-\alpha-2} \frac{A^2 2^\alpha}{B(\alpha-1)^2(\alpha-2)}.
\end{aligned}$$

It is necessary that $\frac{A 2^\alpha}{B(\alpha-1)^2(\alpha-2)} < 1$, so that f^{n+1} satisfies the property (4.16). Then, $xf(x)$ is integrable in $+\infty$ and thus, $f^{n+1} \in \mathcal{B}$. By integrating (4.14), it is easily seen that, if $M_1(f^0) = \sqrt{2v(0)f_0}$ then $\forall n \in \mathbb{N}, M_1(f^n) = \sqrt{2v(0)f_0}$. This property implies weak convergence in the space of measures, so that $f^n \to f_\infty \neq 0$ will converge tightly for a subsequence.

Appendices

Appendix A

Large aggregate limit

We denote by $c_{i,j,k}(t)$ the probability of the aggregate to be in the state (i,j,k) at time t. Its evolution will be determined by a jump process model of the reactions with the rates given in (2.2), (2.3), (2.4), (2.5), (2.6), (2.7), (2.9), and (2.10).

For this purpose the relation between pre-reaction state (i',j',k') and post-reaction state (i,j,k) needs to be inverted. This is easy except for Reaction 5, where we have $j = j' - 1$, $k = k' - 1$, and, with (2.9),

$$i = i' + 1 - \ell_{i',j',k'} = i' + 1 - \left\lfloor \frac{(n-1)i'}{nk' - 2j'} \right\rceil . \tag{A.1}$$

The inversion is not possible in general. Occasionally, $\ell_{i',j',k'}$ will increase by one, when i' is increased by one, implying that i might take the same value for two consecutive values of i'. Even worse: For the extreme case $nk' - 2j' = n - 1$, where after the loss of a p62 oligomer all binding sites are busy with two-hand bound Ubi except the one remaining after breaking the connection, i.e. $nk - 2j = 1 = i$. This state is independent from the number $i' \in \{0, \ldots, n-1\}$ of one-hand bound Ubi getting lost with the oligomer. Therefore we introduce

$$I_{i,j,k} = \{i' : i = i' + 1 - \ell_{i',j+1,k+1}\}$$

The equation for the probability distribution reads

$$\begin{aligned} \frac{dc_{i,j,k}}{dt} \quad = \quad & (r_1 c)_{i-1,j,k} - (r_1 c)_{i,j,k} + (r_2 c)_{i+1,j-1,k-1} - (r_2 c)_{i,j,k} + (r_3 c)_{i+1,j-1,k} - (r_3 c)_{i,j,k} \\ & + (r_{-1} c)_{i+1,j,k} - (r_{-1} c)_{i,j,k} + \sum_{i' \in I_{i,j,k}} (r_{-2} c)_{i',j+1,k+1} - (r_{-2} c)_{i,j,k} \\ & + (r_{-3} c)_{i-1,j+1,k} - (r_{-3} c)_{i,j,k} \, . \end{aligned} \tag{A.2}$$

We introduce a typical value k_0 for the number k of oligomers in the aggregate and use it also as a reference value for i and j, leading by the definition (2.11) to the scaled triplet (p,q,r). The latter lives on a grid with spacing $\Delta p = \Delta q = \Delta r := 1/k_0$ and, thus, becomes a continuous variable in the large aggregate limit $k_0 \to \infty$. Therefore we postulate the existence of a probability density $P(p,q,r,t)$ such that

$$c_{i,j,k}(t) \approx k_0^3 \, P\left(\frac{i}{k_0}, \frac{j}{k_0}, \frac{k}{k_0}, t\right) .$$

Division of (A.2) by k_0^3 and the limit $k_0 \to \infty$ ($\Delta p = \Delta q = \Delta r \to 0$) will lead to an equation for P. We deal with the six differences on the right hand side of (A.2), corresponding to the six reactions, separately.

Reaction 1:

$$\begin{aligned}
&k_0^{-3}\left[(r_1c)_{i-1,j,k}-(r_1c)_{i,j,k}\right]\\
&\approx\frac{1}{\Delta p}\left[\kappa_1(nr-p+\Delta p-2q)P(p-\Delta p,q,r,t)-\kappa_1(nr-p-2q)P(p,q,r,t)\right]\\
&\to-\partial_p(\kappa_1(nr-p-2q)P)\,.
\end{aligned}$$

Reaction 2:

$$\begin{aligned}
&k_0^{-3}\left[(r_2c)_{i+1,j-1,k-1}-(r_2c)_{i,j,k}\right]\\
&\approx\frac{1}{\Delta p}\left[\kappa_2(p+\Delta p)P(p+\Delta p,q-\Delta q,r-\Delta r,t)-\kappa_2pP(p,q-\Delta q,r-\Delta r,t)\right]\\
&\quad+\frac{1}{\Delta q}\left[\kappa_2pP(p,q-\Delta q,r-\Delta r,t)-\kappa_2pP(p,q,r-\Delta r,t)\right]\\
&\quad+\frac{1}{\Delta r}\left[\kappa_2pP(p,q,r-\Delta r,t)-\kappa_2pP(p,q,r,t)\right]\\
&\to\partial_p(\kappa_2pP)-\partial_q(\kappa_2pP)-\partial_r(\kappa_2pP)\,.
\end{aligned}$$

Reaction 3: Since this is a second-order reaction, it would dominate the dynamics for large k_0, if the reaction constant were of the same order of magnitude as the others. In order to avoid this, we set $\kappa_3'=\kappa_3/k_0$ and keep κ_3 fixed as $k_0\to\infty$.

$$\begin{aligned}
&k_0^{-3}\left[(r_3c)_{i+1,j-1,k}-(r_3c)_{i,j,k}\right]\\
&\approx\frac{1}{\Delta p}\big[\kappa_3(p+\Delta p)(nr-p-\Delta p-2q+2\Delta q)P(p+\Delta p,q-\Delta q,r,t)\\
&\qquad-\kappa_3p(nr-p-2q+2\Delta q)P(p,q-\Delta q,r,t)\big]\\
&\quad+\frac{1}{\Delta q}\left[\kappa_3p(nr-p-2q+2\Delta q)P(p,q-\Delta q,r,t)-\kappa_3p(nr-p-2q)P(p,q,r,t)\right]\\
&\to\partial_p(\kappa_3p(nr-p-2q)P)-\partial_q(\kappa_3p(nr-p-2q)P)\,.
\end{aligned}$$

Reaction 4:

$$\begin{aligned}
&k_0^{-3}\left[(r_{-1}c)_{i+1,j,k}-(r_{-1}c)_{i,j,k}\right]\\
&\approx\frac{1}{\Delta p}\left[\kappa_{-1}(p+\Delta p)P(p+\Delta p,q,r,t)-\kappa_{-1}pP(p,q,r,t)\right]\\
&\to\partial_p(\kappa_{-1}pP)\,.
\end{aligned}$$

Reaction 5: As preparatory steps, we compute

$$\ell_{i',j+1,k+1}=\left\lfloor\frac{(n-1)i'}{nk-2j+n-2}\right\rfloor=\left\lfloor\frac{(n-1)p'}{nr-2q+(n-2)\Delta p}\right\rfloor\,.$$

As a function of p', this is piecewise constant and equal to $\left\lfloor\frac{(n-1)p'}{nr-2q}\right\rfloor$ with jumps (for small Δp) close to the set $\frac{nr-2q}{n-1}\left(\frac12+\mathbb{N}_0\right)$. Away from these points the map (A.1) from pre- to post-reaction states is invertible with

$$p'=p+\Delta p\,(\ell(p,q,r)-1)\,,\qquad \ell(p,q,r):=\left\lfloor\frac{(n-1)p}{nr-2q}\right\rfloor\,.$$

Note that p' has been replaced by p in the argument of ℓ since $p-p'=O(\Delta p)$. At all these generic points the sum in (A.2) has only one term. We shall also need

$$\alpha_{j,k}\to\frac{nr-2q}{(n-2)r}=:\alpha(q,r)\,.$$

Thus,

$$
\begin{aligned}
&k_0^{-3}\left[\mathbb{1}_{i\geq 1}(r_{-2}c)_{I_{i,j,k},j+1,k+1}-(r_{-2}c)_{i,j,k}\right]\\
&\approx\frac{1}{\Delta p}\big[\kappa_-\alpha(q+\Delta q,r+\Delta r)(q+\Delta q)P(p+\Delta p(\ell-1),q+\Delta q,r+\Delta,t)\\
&\qquad-\kappa_-\alpha(q+\Delta q,r+\Delta r)(q+\Delta q)P(p,q+\Delta q,r+\Delta r,t)\big]\\
&\approx\frac{1}{\Delta q}\big[\kappa_-\alpha(q+\Delta q,r+\Delta r)(q+\Delta q)P(p,q+\Delta q,r+\Delta,t)\\
&\qquad-\kappa_-\alpha(q,r+\Delta r)qP(p,q,r+\Delta r,t)\big]\\
&\approx\frac{1}{\Delta r}\big[\kappa_-\alpha(q,r+\Delta r)qP(p,q,r+\Delta,t)\\
&\qquad-\kappa_-\alpha(q,r)qP(p,q,r,t)\big]\\
&\to\partial_p(\kappa_-\alpha(\ell-1)qP)+\partial_q(\kappa_-\alpha qP)+\partial_r(\kappa_-\alpha qP)\,.
\end{aligned}
$$

Note that the factor $\ell-1$ has been written inside the derivative since ℓ is constant away from finitely many critical points. We replace a detailed analysis at these points by the simple argument that the equation for P has to be in conservation form to preserve the total probability. Finally we introduce a simplification by dropping the rounding operation in ℓ.

Reaction 6:

$$
\begin{aligned}
&k_0^{-3}\left[(r_{-3}c)_{i+1,j-1,k}-(r_{-3}c)_{i,j,k}\right]\\
&\approx\frac{1}{\Delta p}\big[\kappa_-(1-\alpha(q+\Delta q,r))(q+\Delta q)P(p-\Delta p,q+\Delta q,r,t)\\
&\qquad-\kappa_-(1-\alpha(q+\Delta q,r))(q+\Delta q)P(p,q+\Delta q,r,t)\big]\\
&\quad+\frac{1}{\Delta q}\left[\kappa_-(1-\alpha(q+\Delta q,r))(q+\Delta q)P(p,q+\Delta q,r,t)-\kappa_-(1-\alpha(q,r))qP(p,q,r,t)\right]\\
&\to-\partial_p(\kappa_-(1-\alpha)qP)+\partial_q(\kappa_-(1-\alpha)qP)\,.
\end{aligned}
$$

Collecting our results, the limiting equation for the evolution of P reads

$$
\begin{aligned}
&\partial_t P+\partial_p\left(\left((\kappa_1-\kappa_3 p)(nr-p-2q)-(\kappa_2+\kappa_{-1})p+\kappa_- q\left(1-\frac{(n-1)p}{(n-2)r}\right)\right)P\right)\\
&+\partial_q\left((\kappa_2 p+\kappa_3 p(nr-p-2q)-\kappa_- q)P\right)+\partial_r\left((\kappa_2 p-\kappa_-\alpha q)P\right)=0\,.
\end{aligned}
\tag{A.3}
$$

For deterministic initial conditions of the form $P(p,q,r,0)=\delta(p-p_0)\delta(q-q_0)\delta(r-r_0)$ the state remains deterministic: $P(p,q,r,t)=\delta(p-p(t))\delta(q-q(t))\delta(r-r(t))$, where $(p(t),q(t),r(t))$ solves the initial value problem (3.1).

Bibliography

[1] D. J. Aldous. Deterministic and stochastic models for coalescence (aggregation, coagulation): A review of the mean-field theory for probabilists. *Bernoulli*, 5, 1999.

[2] Liam D. Aubrey, Ben J. F. Blakeman, Liisa Lutter, Christopher J. Serpell, Mick F. Tuite, Louise C. Serpell, and Wei-Feng Xue. Quantification of amyloid fibril polymorphism by nano-morphometry reveals the individuality of filament assembly. *bioRxiv*, 2020.

[3] J. Banasiak and W. Lamb. On a coagulation and fragmentation equation with mass loss. *Proc. Roy. Soc. Edinburgh Sect. A*, 136(6):1157–1173, 2006.

[4] Jacek Banasiak and Wilson Lamb. Global strict solutions to continuous coagulation-fragmentation equations with strong fragmentation. *Proceedings of the Royal Society of Edinburgh: Section A Mathematics*, 141(3):465–480, 2011.

[5] R. Becker and W. Döring. Kinetische behandlung der keimbildung in übersättigten dämpfen. *Annalen der Physik*, 416(8):719–752, 1935.

[6] M.F. Bishop and F.A. Ferrone. Kinetics of nucleation-controlled polymerization. a perturbation treatment for use with a secondary pathway. *Biophys. J.*, 46(5):631 – 644, 1984.

[7] Geir Bjørkøy, Trond Lamark, Andreas Brech, Heidi Outzen, Maria Perander, Aud Overvatn, Harald Stenmark, and Terje Johansen. p62/sqstm1 forms protein aggregates degraded by autophagy and has a protective effect on huntingtin-induced cell death. *The Journal of cell biology*, 171(4):603–614, 11 2005.

[8] Jean-Pierre Bourgade and Francis Filbet. Convergence of a finite volume scheme for coagulation-fragmentation equations. *Mathematics of Computation*, 77:851–882, 2008.

[9] Carmen Chicone. *Ordinary Differential Equations with Applications*, volume 34. Springer-Verlag New York, 1999.

[10] Monique Chyba, Jakob Kotas, Vincent Beringue, Christopher Eblen, Angelique Igel-Egalon, Yuliia Kravchenko, and Human Rezaei. An alternative model to prion fragmentation based on the detailed balance between prpsc and suprp. *bioRxiv*, 2020.

[11] Jean-Pierre Françoise. *Oscillations en biologie*, volume 46. Springer-Verlag Berlin Heidelberg, 2005.

[12] J.-F. Collet, T. Goudon, F. Poupaud, and A. Vasseur. The Becker–Döring system and its Lifshitz–Slyozov limit. *SIAM J. on Appl. Math.*, 62(5):1488–1500, 2002.

[13] A. Danieli and S. Martens. p62-mediated phase separation at the intersection of the ubiquitin-proteasome system and autophagy. *Journal of Cell Science*, 131(19), 2018.

[14] J. Delacour, M. Doumic, S. Martens, C. Schmeiser, and G. Zaffagnini. A mathematical model of p62-ubiquitin aggregates in autophagy. arXiv:2004.07926.

[15] Vojo Deretic, Tomonori Kimura, Graham Timmins, Pope Moseley, Santosh Chauhan, and Michael Mandell. Immunologic manifestations of autophagy. *The Journal of Clinical Investigation*, 125(1):75–84, 1 2015.

[16] Laurent Desvillettes and Klemens Fellner. Duality- and entropy methods in coagulation-fragmentation models. *Riv. Mat. Univ. Parma (N.S.)*, 4(2):215–263, 2013.

[17] Marie Doumic, Klemens Fellner, Mathieu Mezache, and Human Rezaei. A bi-monomeric, nonlinear Becker-Döring-type system to capture oscillatory aggregation kinetics in prion dynamics. working paper or preprint, August 2018.

[18] P.B. Dubovskiĭ and I.W. Stewart. Existence, uniqueness and mass conservation for the coagulation-fragmentation equation. *Math. Methods Appl. Sci.*, 19(7):571–591, 1996.

[19] P. B. Dubovskiĭ and I. W. Stewart. Trend to equilibrium for the coagulation–fragmentation equation. *Mathematical Methods in the Applied Sciences*, 19(10):761–772, 1996.

[20] F. Dumortier. Techniques in the theory of local bifurcations: Blow-up, normal forms, nilpotent bifurcations, singular perturbations. In *Bifurcations and Periodic Orbits of Vector Fields*, pages 19–73. Kluwer Acad. Publ., 1993.

[21] M. Escobedo, Ph. Laurençot, S. Mischler, and B. Perthame. Gelation and mass conservation in coagulation-fragmentation models. *Journal of Differential Equations*, 195(1):143 – 174, 2003.

[22] M. Escobedo, S. Mischler, and B. Perthame. Gelation in coagulation and fragmentation models. *Communications in Mathematical Physics*, 231(1):157–188, 2002.

[23] M. Escobedo, S. Mischler, and M. [Rodriguez Ricard]. On self-similarity and stationary problem for fragmentation and coagulation models. *Annales de l'Institut Henri Poincare (C) Non Linear Analysis*, 22(1):99 – 125, 2005.

[24] N. Fenichel. Geometric singular perturbation theory for ordinary differential equations. *Journal of Differential Equations*, 31:53–98, 1979.

[25] Francis Filbet and Philippe Laurençot. Numerical simulation of the smoluchowski coagulation equation. *SIAM J. Sci. Comput.*, 25(6):2004–2028, June 2004.

[26] Joan C. Artes Freddy Dumortier, Jaume Llibre. *Qualitative Theory of Planar Differential Systems*. Springer International Publishing, 2006.

[27] A. Frieze and M. Karonski. *Introduction to Random Graphs*. Cambridge University Press, Cambridge, 2015.

[28] L. Galluzzi, J.M. Bravo-San Pedro, and G. Kroemer. Defective autophagy initiates malignant transformation. *Molecular Cell*, 62(4):473–474, 2018/09/10 2016.

[29] Thierry Goudon, Frederic Lagouttiere, and Leon Matar Tine. Simulations of the lifshitz-slyozov equations : the role of coagulation terms in the asymptotic behavior. *Mathematical Models and Methods in Applied Sciences*, 23(07):1177–1215, 2013.

[30] Taichi Hara, Kenji Nakamura, Makoto Matsui, Akitsugu Yamamoto, Yohko Nakahara, Rika Suzuki-Migishima, Minesuke Yokoyama, Kenji Mishima, Ichiro Saito, Hideyuki Okano, and Noboru Mizushima. Suppression of basal autophagy in neural cells causes neurodegenerative disease in mice. *Nature*, 441(7095):885–889, 2006.

[31] Masaaki Komatsu, Satoshi Waguri, Masato Koike, Yu shin Sou, Takashi Ueno, Taichi Hara, Noboru Mizushima, Jun ichi Iwata, Junji Ezaki, Shigeo Murata, Jun Hamazaki, Yasumasa Nishito, Shun ichiro Iemura, Tohru Natsume, Toru Yanagawa, Junya Uwayama, Eiji Warabi, Hiroshi Yoshida, Tetsuro Ishii, Akira Kobayashi, Masayuki Yamamoto, Zhenyu Yue, Yasuo Uchiyama, Eiki Kominami, and Keiji Tanaka. Homeostatic levels of p62 control cytoplasmic inclusion body formation in autophagy-deficient mice. *Cell*, 131(6):1149 – 1163, 2007.

[32] J Kopitz, G O Kisen, P B Gordon, P Bohley, and P O Seglen. Nonselective autophagy of cytosolic enzymes by isolated rat hepatocytes. *The Journal of cell biology*, 111(3):941–953, 09 1990.

[33] V.M. Krishnamurthy, L.A. Estroff, and G.M. Whitesides. *Multivalency in Ligand Design*, chapter 2, pages 11–53. Wiley-Blackwell, 2006.

[34] Christian Kuehn. *Multi time scale dynamics*, volume 191. Springer International Publishing, 2015.

[35] P. Laurençot and S. Mischler. From the discrete to the continuous coagulation-fragmentation equations. *Proc. Roy. Soc. Edinburgh Sect. A*, 132(5):1219–1248, 2002.

[36] Philippe Laurençot. Stationary solutions to coagulation-fragmentation equations. *Annales de l'Institut Henri Poincaré C, Analyse non linéaire*, 36(7):1903 – 1939, 2019.

[37] Philippe Laurençot and Stéphane Mischler. Convergence to equilibrium for the continuous coagulation-fragmentation equation. *Bulletin des Sciences Mathématiques*, 127(3):179 – 190, 2003.

[38] B. Levine and G. Kroemer. Autophagy in the pathogenesis of disease. *Cell*, 132(1):27–42, 01 2008.

[39] J. Long, T.P. Garner, M.J. Pandya, C.J. Craven, P. Chen, B. Shaw, M.P. Williamson, R. Layfield, and M.S. Searle. Dimerisation of the uba domain of p62 inhibits ubiquitin binding and regulates nf-kappab signalling. *J. Mol. Biol.*, 396(1):178—194, February 2010.

[40] G. Menon and Robert L. Pego. Approach to self-similarity in smoluchowski's coagulation equations. arXiv:nlin/0306047, 2003.

[41] Hitoshi Nakatogawa, Kuninori Suzuki, Yoshiaki Kamada, and Yoshinori Ohsumi. Dynamics and diversity in autophagy mechanisms: lessons from yeast. *Nature Reviews Molecular Cell Biology*, 10(7):458–467, 2009.

[42] R.A. Nixon and D.-S. Yang. Autophagy failure in alzheimer's disease—locating the primary defect. *Neurobiology of Disease*, 43(1):38 – 45, 2011. Autophagy and protein degradation in neurological diseases.

[43] Yusuke O., Tomoya M., Kosuke A., Kenichi Nakajima, Atsushi Masuyama, Hiromasa Goto, Yuya Nishida, Takeshi Miyatsuka, Yoshio Fujitani, Masato Koike, Masako Mitsumata, and Hirotaka Watada. Defective autophagy in vascular smooth muscle cells enhances cell death and atherosclerosis. *Autophagy*, 0(0):1–16, 2018. PMID: 30025494.

[44] Laura D Osellame and Michael R Duchen. Defective quality control mechanisms and accumulation of damaged mitochondria link gaucher and parkinson diseases. *Autophagy*, 9(10):1633–1635, 2013. PMID: 23989665.

[45] S. Pankiv, T.H. Clausen, T. Lamark, A. Brech, J.-A. Bruun, H. Outzen, A. Ø vervatn, G. Bjø rkøy, and T. Johansen. p62/sqstm1 binds directly to atg8/lc3 to facilitate degradation of ubiquitinated protein aggregates by autophagy. *J. Biol. Chem.*, 282(33):24131–24145, 2007.

[46] Lawrence Perko. *Differential Equations and dynamical systems*, volume 7. Springer-Verlag New York, 2001.

[47] H. Poincaré. Mémoire sur les courbes définies par une équation différentielle (i). *Journal de mathématiques pures et appliquées 3^e série, tome 7*, pages 375–422, 1881.

[48] S. Prigent, A. Ballesta, F. Charles, N. Lenuzza, P. Gabriel, L.M. Tine, H. Rezaei, and M. Doumic. An efficient kinetic model for assemblies of amyloid fibrils and its application to polyglutamine aggregation. *PLOS ONE*, 7(11):1–9, 11 2012.

[49] M. Reed and B. Simon. *II: Fourier Analysis, Self-Adjointness*. Methods of Modern Mathematical Physics. Elsevier Science, 1975.

[50] Drake R.L. *Topics in Current Aerosol Research*, volume 3. Pergamon Press, 1972.

[51] Vladimir Rogov, Volker Dötsch, Terje Johansen, and Vladimir Kirkin. Interactions between autophagy receptors and ubiquitin-like proteins form the molecular basis for selective autophagy. *Molecular Cell*, 53(2):167 – 178, 2014.

[52] C. Schmeiser and R. Weiß. Asymptotic analysis of singular singularly perturbed boundary value problems. *SIAM J. Math. Anal.*, 17:560–579, 1986.

[53] Konrad Schmüdgen. *The moment problem*, volume 277. Springer International Publishing, 2017.

[54] M. v. Smoluchowski. Drei vorträge über diffusion, brownsche molekularbewegung und koagulation von kolloidteilchen. *Phys. Z.*, 17, 1916.

[55] D. Sun, R. Wu, J. Zheng, P. Li, and L. Yu. Polyubiquitin chain-induced p62 phase separation drives autophagic cargo segregation. *Cell Research*, 28(4):405–415, 2018.

[56] P. Szmolyan. Transversal heteroclinic and homoclinic orbits in singular perturbation problems. *Journal of Differential Equations*, 92:252–281, 1991.

[57] Akito Takamura, Masaaki Komatsu, Taichi Hara, Ayako Sakamoto, Chieko Kishi, Satoshi Waguri, Yoshinobu Eishi, Okio Hino, Keiji Tanaka, and Noboru Mizushima. Autophagy-deficient mice develop multiple liver tumors. *Genes & development*, 25(8):795–800, 04 2011.

[58] A. N. Tikhonov. Systems of differential equations containing small parameters in the derivatives. *Matematicheskii sbornik*, 73:575–586, 1952.

[59] B. Wurzer, G. Zaffagnini, D. Fracchiolla, E. Turco, C. Abert, J. Romanov, and S. Martens. Oligomerization of p62 allows for selection of ubiquitinated cargo and isolation membrane during selective autophagy. *eLife*, 4:e08941, sep 2015.

[60] W.-F. Xue, S.W. Homans, and S.E. Radford. Systematic analysis of nucleation-dependent polymerization reveals new insights into the mechanism of amyloid self-assembly. *PNAS*, 105:8926–8931, 2008.

[61] G. Zaffagnini. *The molecular mechanism of human cargo receptor p62 during selective autophagy.* PhD thesis, University of Vienna, 2016.

[62] G. Zaffagnini, A. Savova, A. Danieli, J. Romanov, S. Tremel, M. Ebner, T. Peterbauer, M. Sztacho, R. Trapannone, A.K. Tarafder, C. Sachse, and S. Martens. p62 filaments capture and present ubiquitinated cargos for autophagy. *The EMBO Journal*, 37(5):e98308, 03 2018.

[63] G. Zaffagnini, A. Savova, A. Danieli, J. Romanov, S. Tremel, M. Ebner, T. Peterbauer, M. Sztacho, R. Trapannone, A.K. Tarafder, C. Sachse, and S. Martens. p62 filaments capture and present ubiquitinated cargos for autophagy. *The EMBO Journal*, 37(5):e98308, 03 2018.

[64] Gabriele Zaffagnini and Sascha Martens. Mechanisms of selective autophagy. *Journal of Molecular Biology*, 428(9, Part A):1714 – 1724, 2016. Molecular Mechanisms of Autophagy, Part A.

[65] Gabriele Zaffagnini, Adriana Savova, Alberto Danieli, Julia Romanov, Shirley Tremel, Michael Ebner, Thomas Peterbauer, Martin Sztacho, Riccardo Trapannone, Abul K Tarafder, Carsten Sachse, and Sascha Martens. p62 filaments capture and present ubiquitinated cargos for autophagy. *The EMBO Journal*, 37(5):e98308, 2018.

Kurzfassung

Das Ziel dieser Dissertation ist die Modellierung der Aggregation von mit Ubiquitin dekoriertem Zellabfall durch Oligomere des Proteins p62, einem wichtigen Schritt in der Vorbereitung zellulärer Autophagie. Ein neues mathematisches Modell für die Dynamik dieser heterogenen Aggregate in der Form eines Systems gewïhnlicher Differentialgleichungen wird hergeleitet und analysiert. Der wesentliche Beitrag dieses neuen Modells liegt in der Tatsache, dass zwei verschiedene Arten von Teilchen berücksichtigt werden, nämlich p62- und Ubiquitin-Moleküle, die Verbindungen sehr spezifischer Art eingehen, was das Komplexitätsniveau des Modells im Vergleich zu klassischen Aggregationsprozessen drastisch erhöht. Im ersten Teil der Arbeit werden drei Parameterbereiche identifiziert, wo Aggregate entweder instabil sind, oder ihre Größe einem endlichen Grenzwert zustrebt, oder ihre Größe ohne Schranken wächst, solange freie Teilchen verfügbar sind. Die Grenzen dieser Parameterbereiche sowie der erwähnte Grenzwert im zweiten Fall werden explizit berechnet. Das Wachstum im dritten Fall (quadratisch mit der Zeit) kann mit Hilfe formaler asymptotischer Methoden ebenso explizit beschrieben werden. Diese qualitativen Resultate werden durch numerische Simulationen illustriert. Ein Vergleich mit experimentellen Resultaten erlaubt eine teilweise Parametrisierung des Modells. Im zweiten Teil der Arbeit werden Methoden aus der Theorie der dynamischen Systeme verwendet, um einige der beobachteten Stabilitätseigenschaften rigoros zu rechtfertigen. Die Instabilität kleiner Aggregate, äquivalent zur Stabilität der Nulllösung, wird mit Hilfe von Blow-up-Methoden bewiesen. Im Beweis des quadratischen Wachstums wird die geometrische Theorie singulärer Störungen verwendet. Der dritte Teil der Arbeit widmet sich einer Erweiterung des Modells, in der Verteilungen von Aggregaten beschrieben werden, deren Wachstum wieder durch das oben erwähnte Modell beschrieben wird, die aber auch einem Koagulationsprozess unterliegen. Das Resultat ist eine komplexe partielle Integro-Differentialgleichung, deren Dimension durch eine Mehr-Skalen-Asymptotik reduziert wird. Die Arbeit wird durch erste Resultate zur Existenz nichttrivialer stationärer Lösungen abgeschlossen.

Abstract

This thesis aims to model the aggregation of ubiquitinated cargo by oligomers of the protein p62, which is an important preparatory step in cellular autophagy. A new mathematical model for the dynamics of these heterogeneous aggregates in the form of a system of ordinary differential equations is derived and analyzed. The main contribution of this new model lies on the fact that we are considering two different particles, namely p62 and Ubiquitin, attaching to each other in a very specific way, which increases drastically the complexity level of the model compared to classical ones. In a first part, three different parameter regimes are identified, where either aggregates are unstable, or their size saturates at a finite value, or their size grows indefinitely as long as free particles are abundant. The boundaries of these regimes as well as the finite size in the second case can be computed explicitly. The growth in the third case (quadratic in time) can also be made explicit by formal asymptotic methods. The qualitative results are illustrated by numerical simulations. A comparison with recent experimental results permits a partial parametrization of the model. In a second part, a partial analysis of this model using dynamical systems tools is also made. The local stability of the regime where the aggregates are unstable is proved using blow-up. The locally quadratic growth in the third regime is also proved using geometric singular perturbation analysis. The end of the thesis is dedicated to the improvement of the former model. Based on biological observations, a coagulation term is added, which leads to a prohibitively complex growth-coagulation model. This is why a simplified version based on a multiscale analysis is formulated where aggregates are only described by one parameter. To conclude, a first basic study of unidimensional growth-coagulation equations is made.